GAMMA-RAY OBSERVATIONS TOWARDS CYGNUS REGION

Ruizhi Yang
on behalf of LHAASO collaboration

BACKGROUND

YMCS

Westerlund 2 (HST image)

NGC 3603 (VLT image)

- More than dozens of OB stars and WRs
- Compact structures (~ pc)

YMCS IN OUR GALAXY

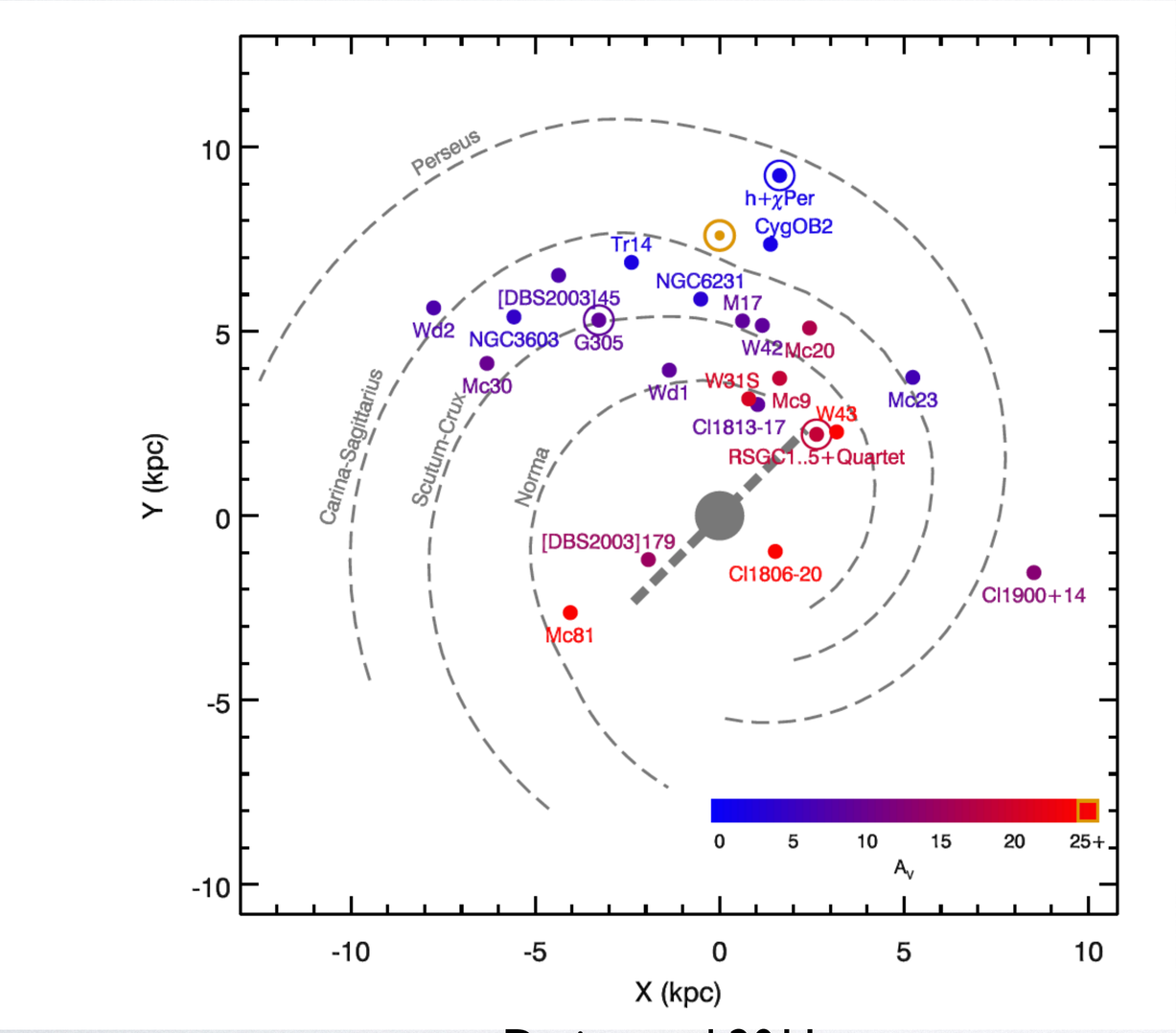

Davies et.al 2011

- ~20 in our Galaxy
- More to be discovered (high extinction in Galactic plane)

Stellar type	$\log[\dot{M}]$ $M_\odot\ yr^{-1}$	V_∞ [km s^{-1}]
WNL	-4.2	1650
WNE	-4.5	1900
WC6-9	-4.4	1800
WC4-5	-4.7	2800
WO	-5.0	3500
O3	-5.2	3190
O4	-5.4	2950
O4.5	-5.5	2900
O5	-5.6	2875

- The wind power of a single young star can be as high as 1e37 erg/s

YMCS CAN POTENTIALLY ACCELERATE CRS

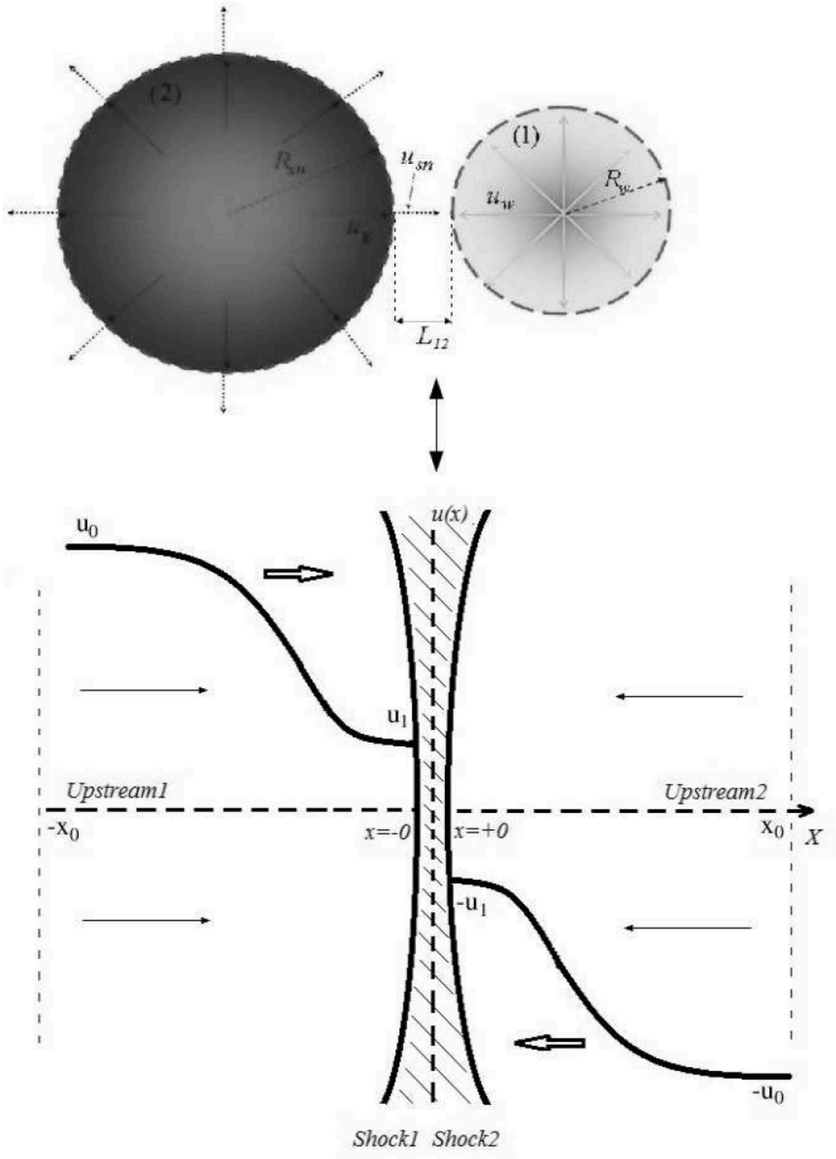

Bykov et.al 2014

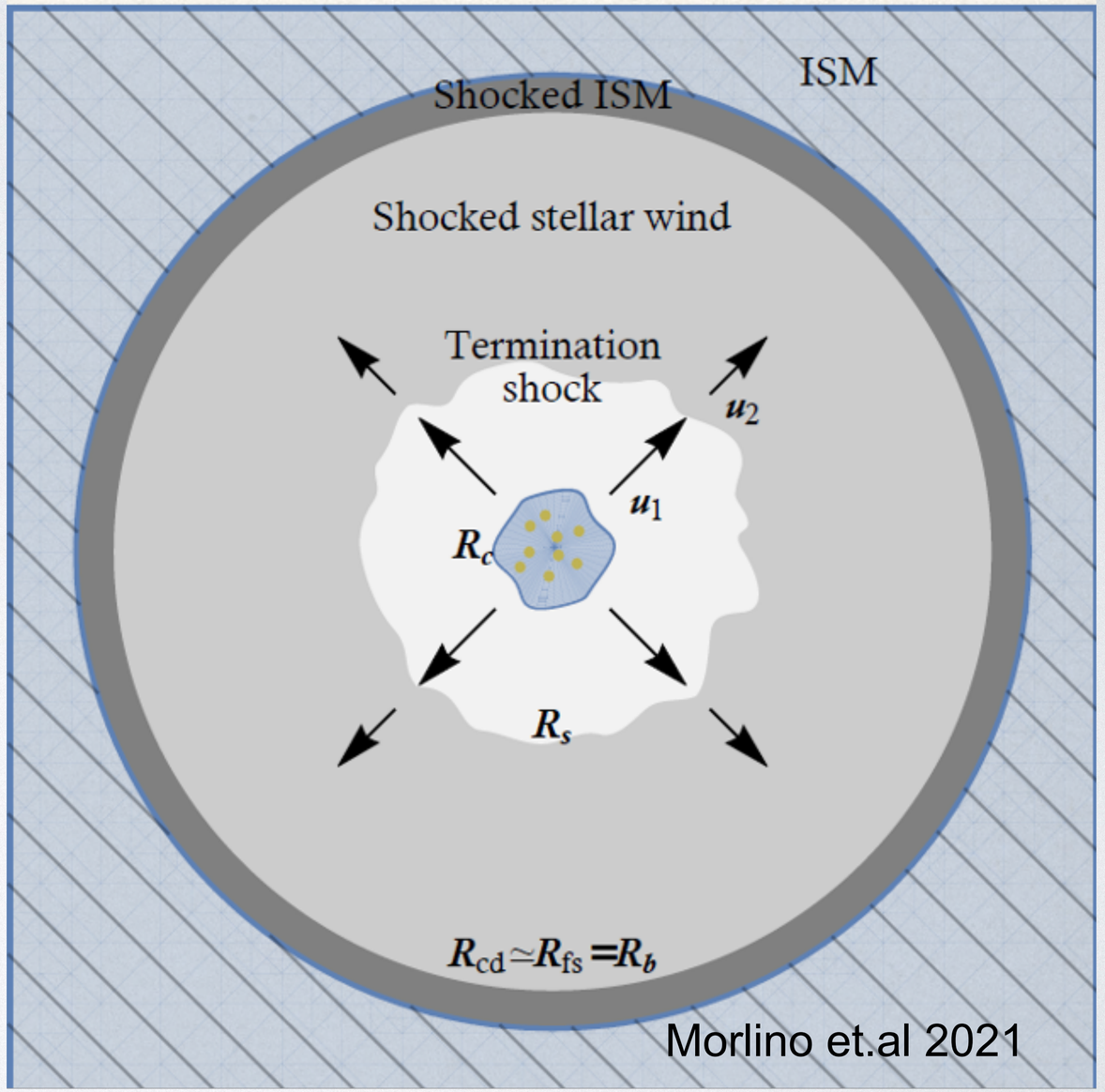

Morlino et.al 2021

YMCS CAN POTENTIALLY ACCELERATE CRS

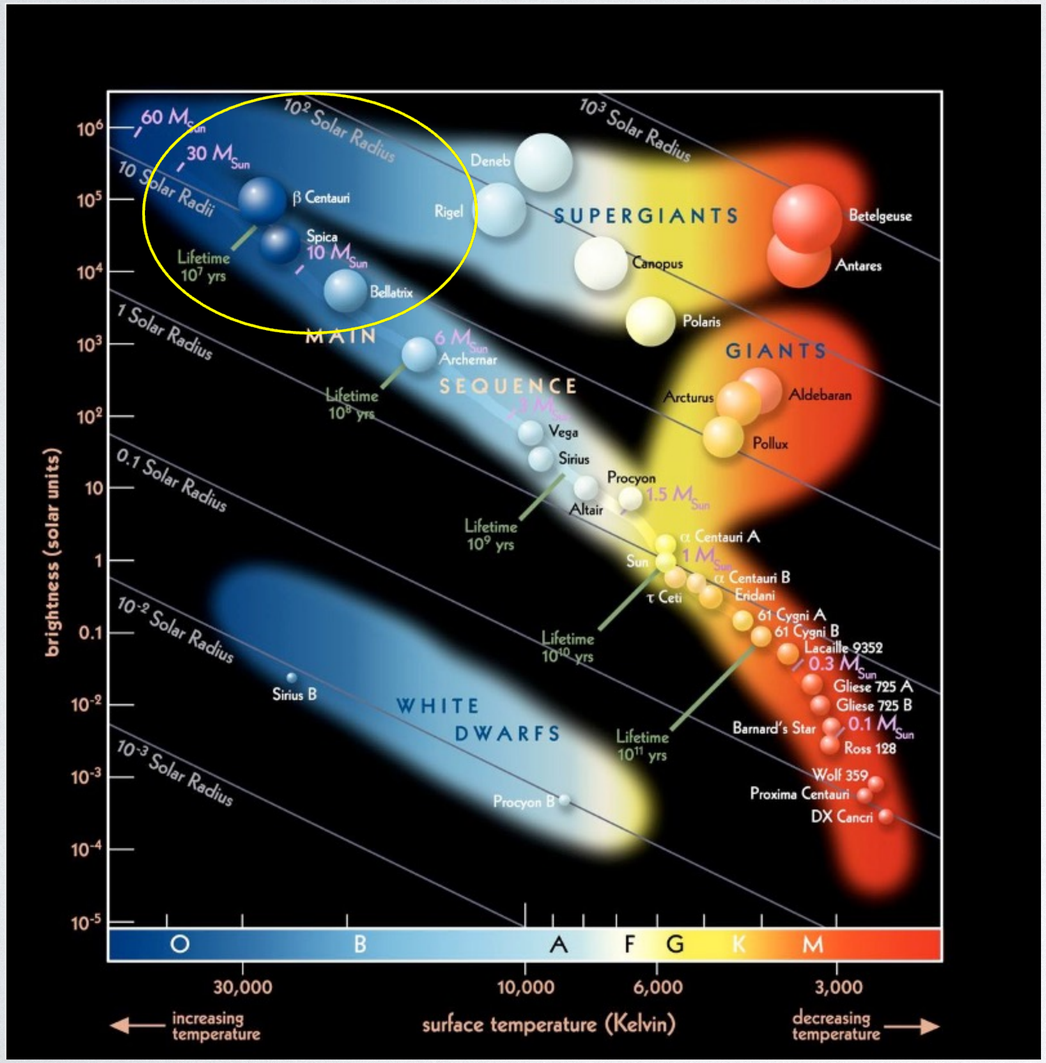

Massive stellar winds as CR accelerators

TABLE 1 — Casse & Paul 1980

DISTANCES BETWEEN THE SHOCK AND THE STAR FOR DIFFERENT KINDS OF STARS IN DIFFERENT ENVIRONMENTS

Distance between the shock and the star (pc)	18	5.2	5.7	1.6
Star:				
Mass loss rate ($M_\odot$ yr^{-1})	10^{-5}	10^{-5}	10^{-6}	10^{-6}
Wind velocity (km s^{-1})	2000	2000	2000	2000
Surrounding medium:				
Density n (particles cm^{-3})	1	10^3	1	10^3
Temperature[a] (K)	10^4	20	10^5	20
Magnetic field strength (μG)	3	30	3	30
Cosmic ray energy density (eV cm^{-3})	1	1	1	1
Pressure (10^{-12} dynes cm^{-2}):				
Due to gas: p_G	2.8	2.8	2.8	2.8
Due to magnetic field: p_B	0.36	36	0.36	36
Due to cosmic rays: p_{CR}	0.15	0.15	0.15	0.15
Total due to ISM: p_t	3.3	39	3.3	39

Provided the acceleration is not intermittent, and in the optimum case, the highest energies that cosmic rays of charge Z can attain at stellar wind terminal shock are:

$$E_{\max} = 4 \times 10^6 \, Z (B/10^{-5}\ \mathrm{G}) \, (w/2.5 \times 10^8\ \mathrm{cm\ s^{-1}})^2\ \mathrm{GeV}$$

whereas for supernova shocks, under similar conditions:

$$E_{\max} < 10^5 \, Z (B/10^{-6}\ \mathrm{G})\ \mathrm{GeV}\,,$$

Cesarsky & Montemerle 1983

GAMMA-RAY EMITTING YMCS

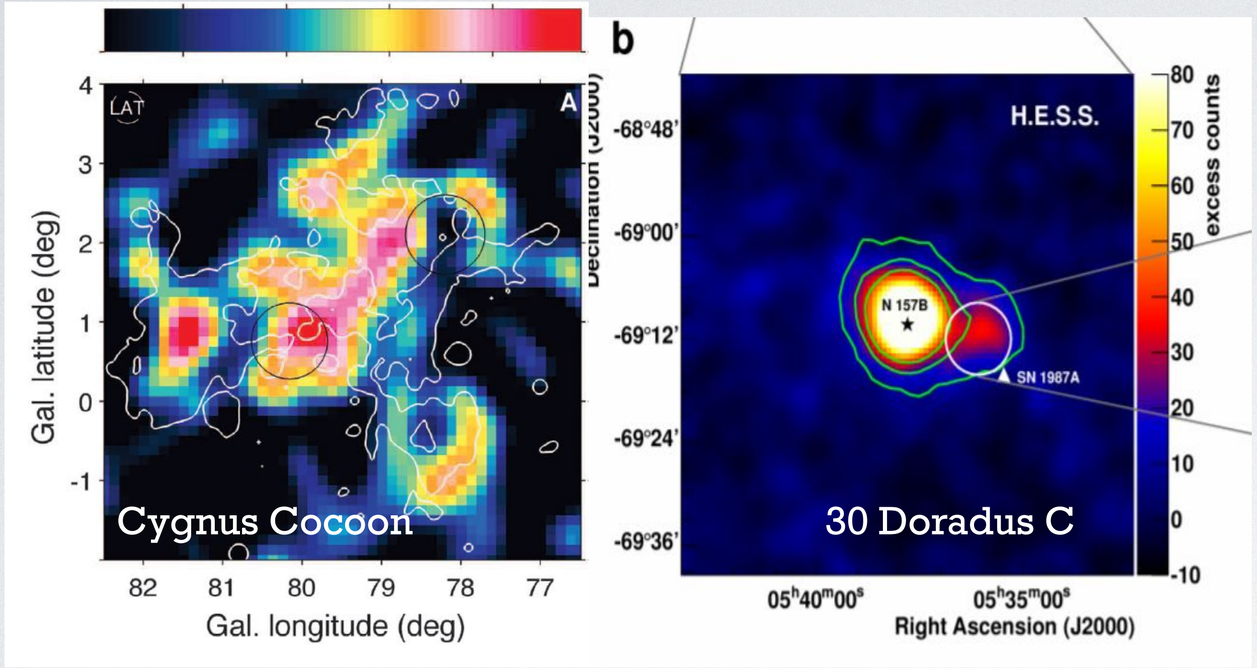

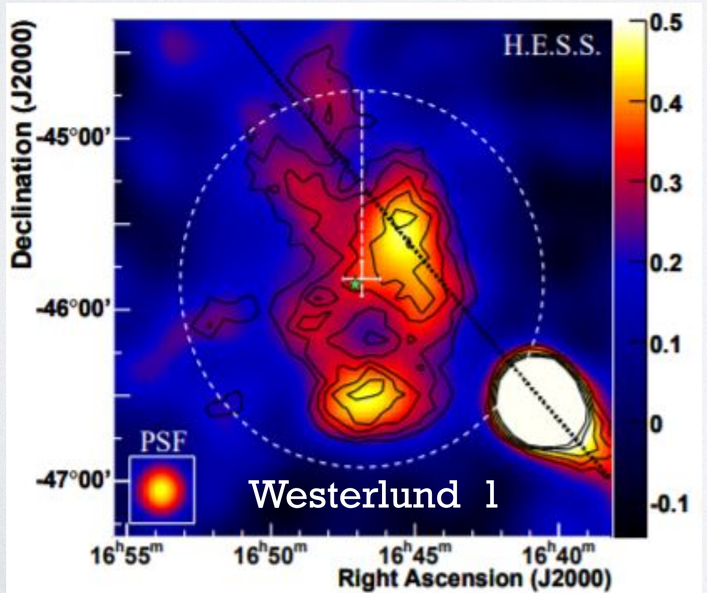

New GAMMA-RAY Source population:

Cygnus Cocoon(GeV-TeV)[Fermi 2012, HAWC2022]
Westerlund 1 (TeV) [HESS collaboration 2012]
Westerlund 2 (GeV, TeV?)[Yang et.al 2018]
NGC 3603 (GeV, TeV)[Yang et.al 2017]
W43 (GeV, TeV?) [Yang et.al 2020]
W40 (GeV) [Sun et.al 2019]
G25/RSGC 1[Sun et.al 2020]
Carina nebular [Ge et.al 2022]
M17 [Liu et.al 2022]

GALACTIC CENTER (HESS 2016)

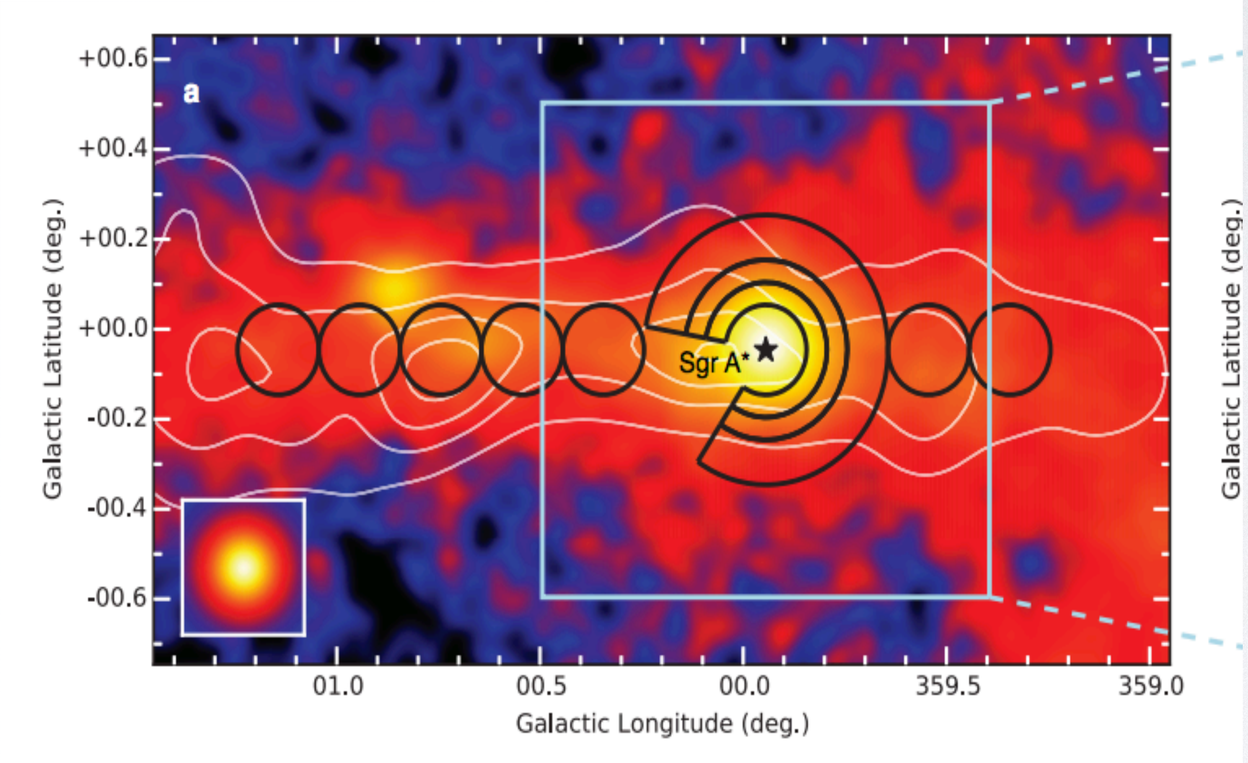

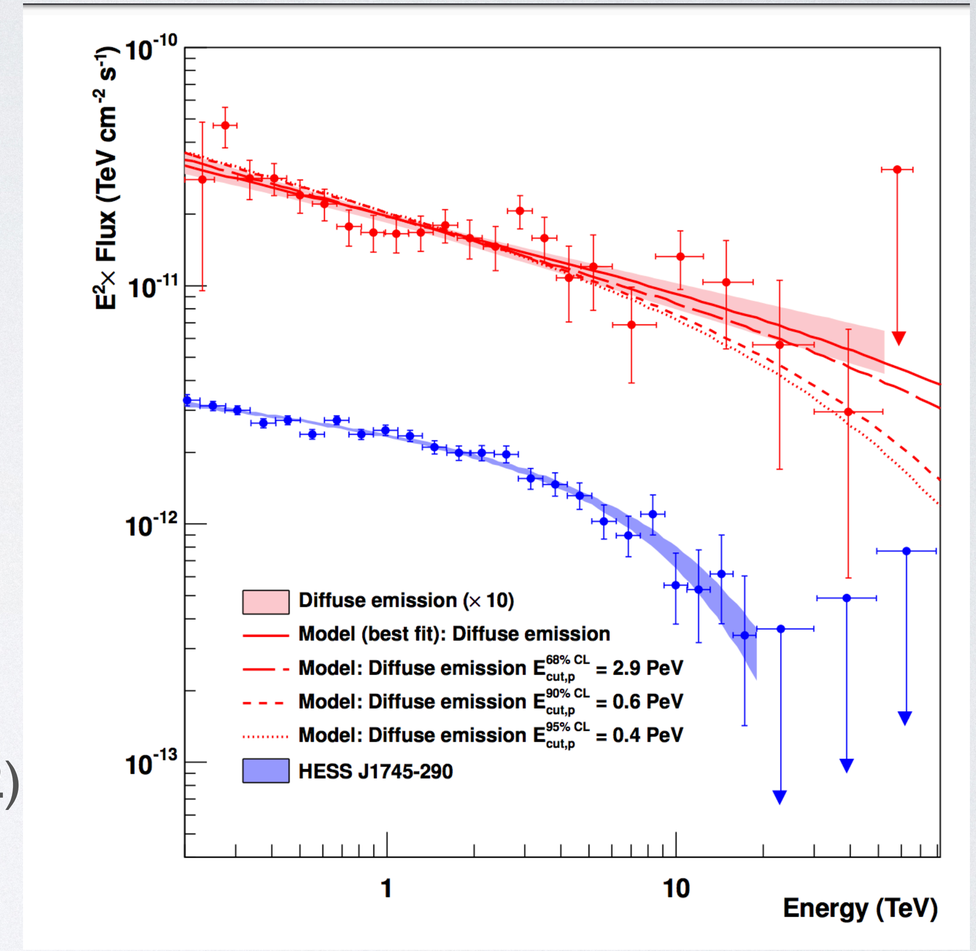

- Also reveal extended emission and hard spectrum (index ~ 2.2)
- Diffuse emission up to more than 150 pc
- GC region harbors Arches, Quintuplet and Nuclear cluster

WESTERLUND 1 FROM H.E.S.S

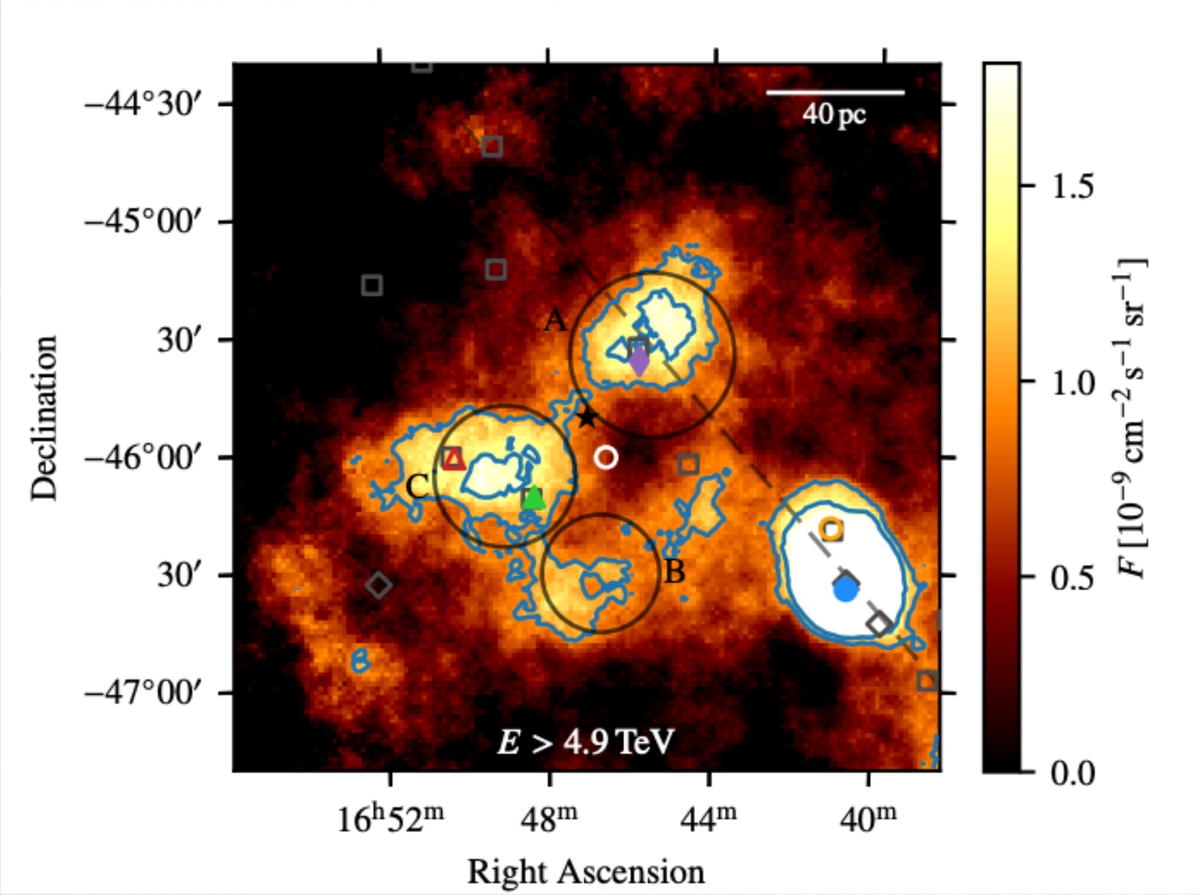

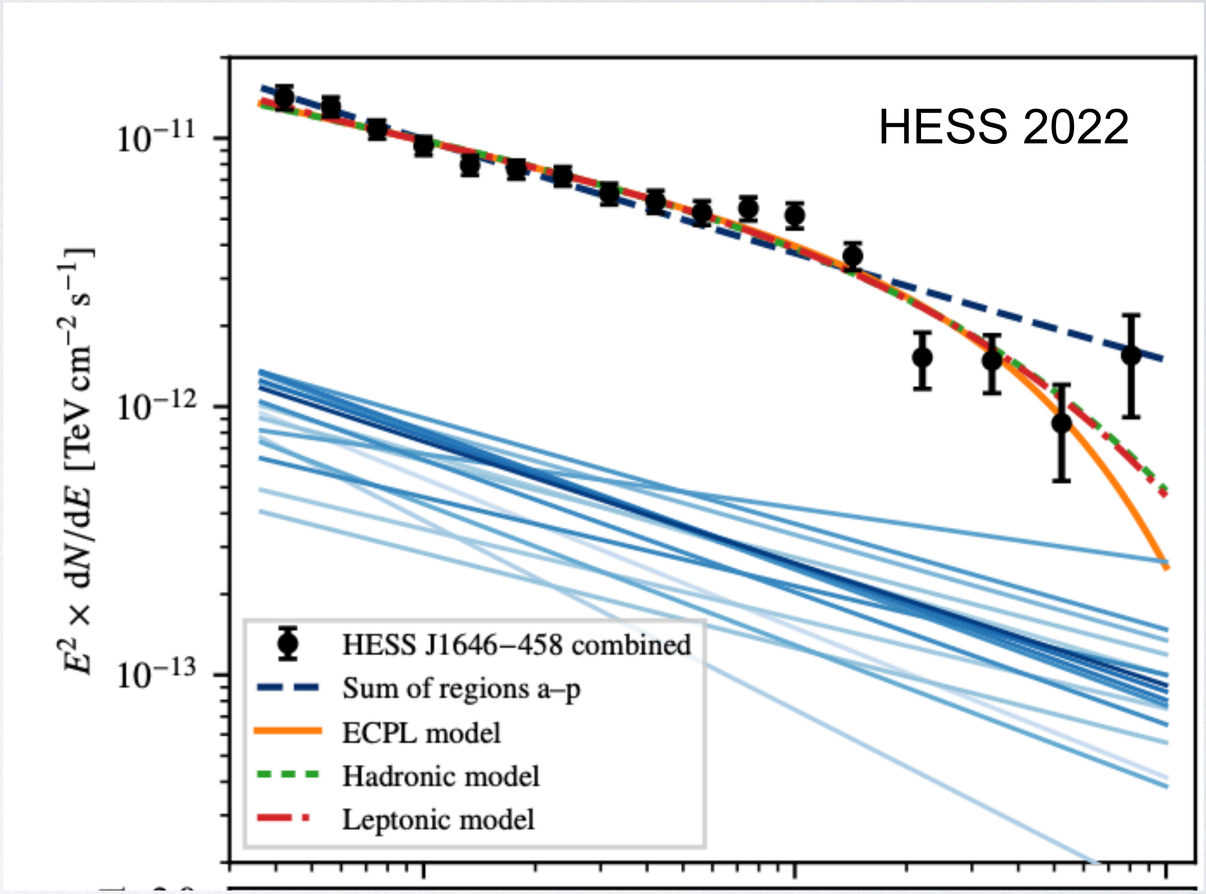

- extended emission up to more than 150 pc
- Hard spectrum up to 20 TeV

RADIAL DISTRIBUTION OF COSMIC RAYS

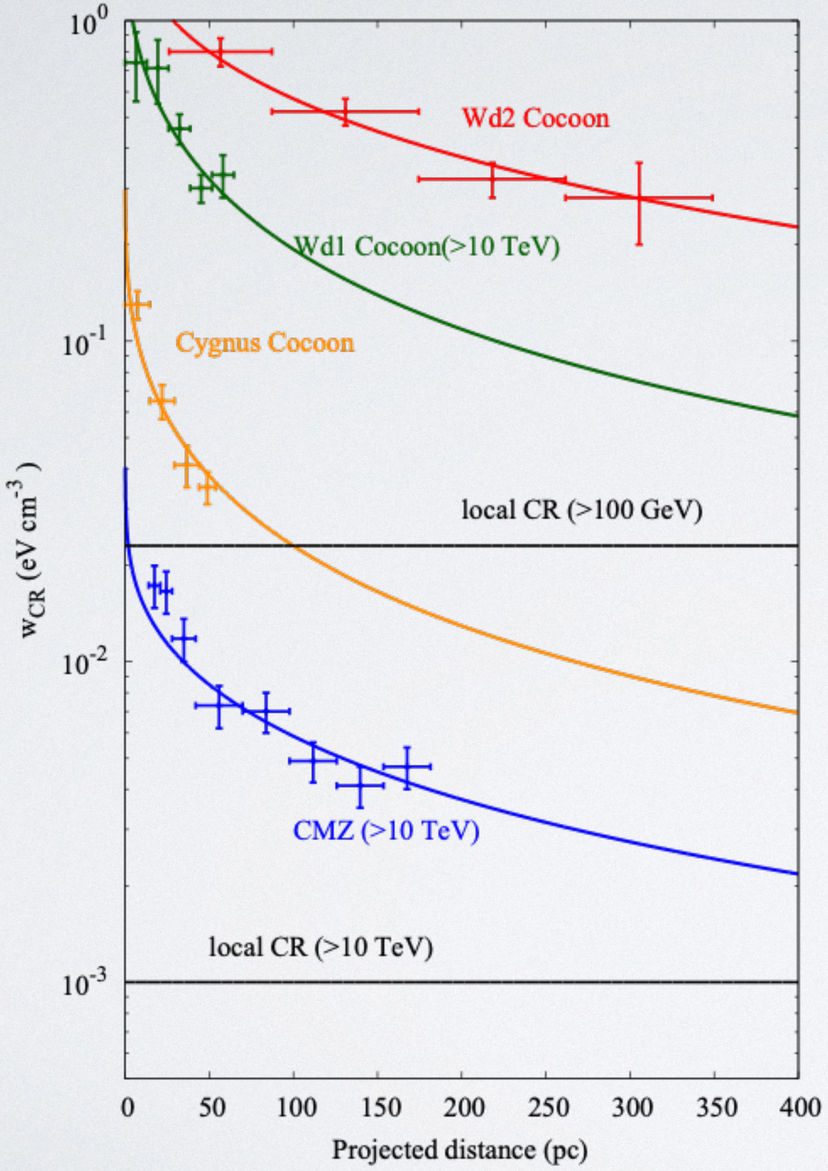

- CR distribution derived by gamma-ray profile and gas distributions
- All four sources (Wd1, Wd2, Cygnus cocoon, GC) show 1/r distribution of CRs
- In diffusion, 1/r profile implies a continuous injection (in the lifetime of clusters)

MASSIVE STAR CLUSTERS AS PEVATRONS?

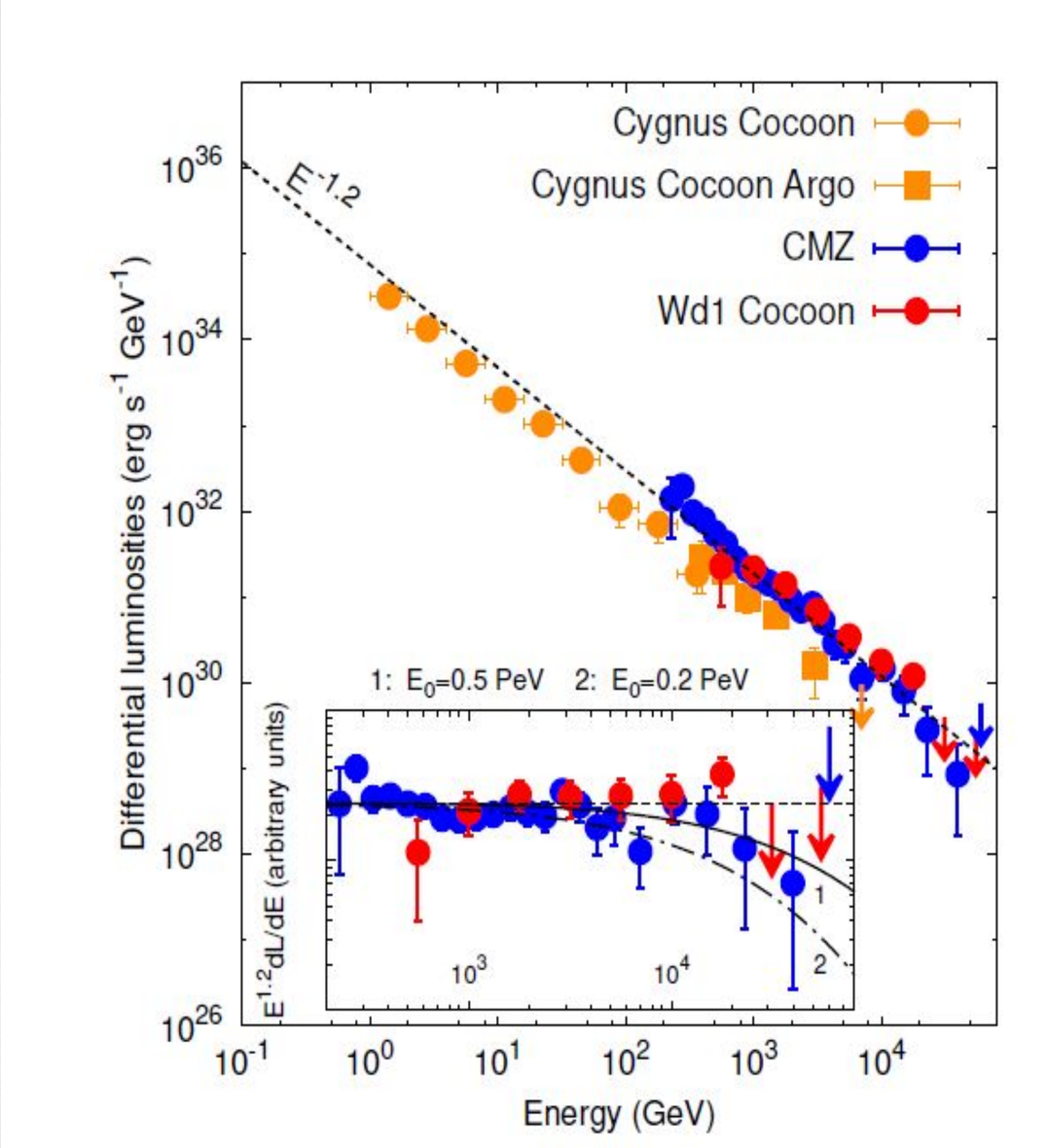

- Cygnus cocoon, Wd 1 and CMZ all emit multi-TeV gamma-ray.
- The spectrum of CMZ and Wd1 put lower limit of cutoff of parent proton spectrum to be several hundred TeV
- Difficult for IACT (large size, UHE)
- LHAASO is the ideal instrument!

CYGNUS REGION

FERMI LAT DETECTION

Fermi Collaboration 2011

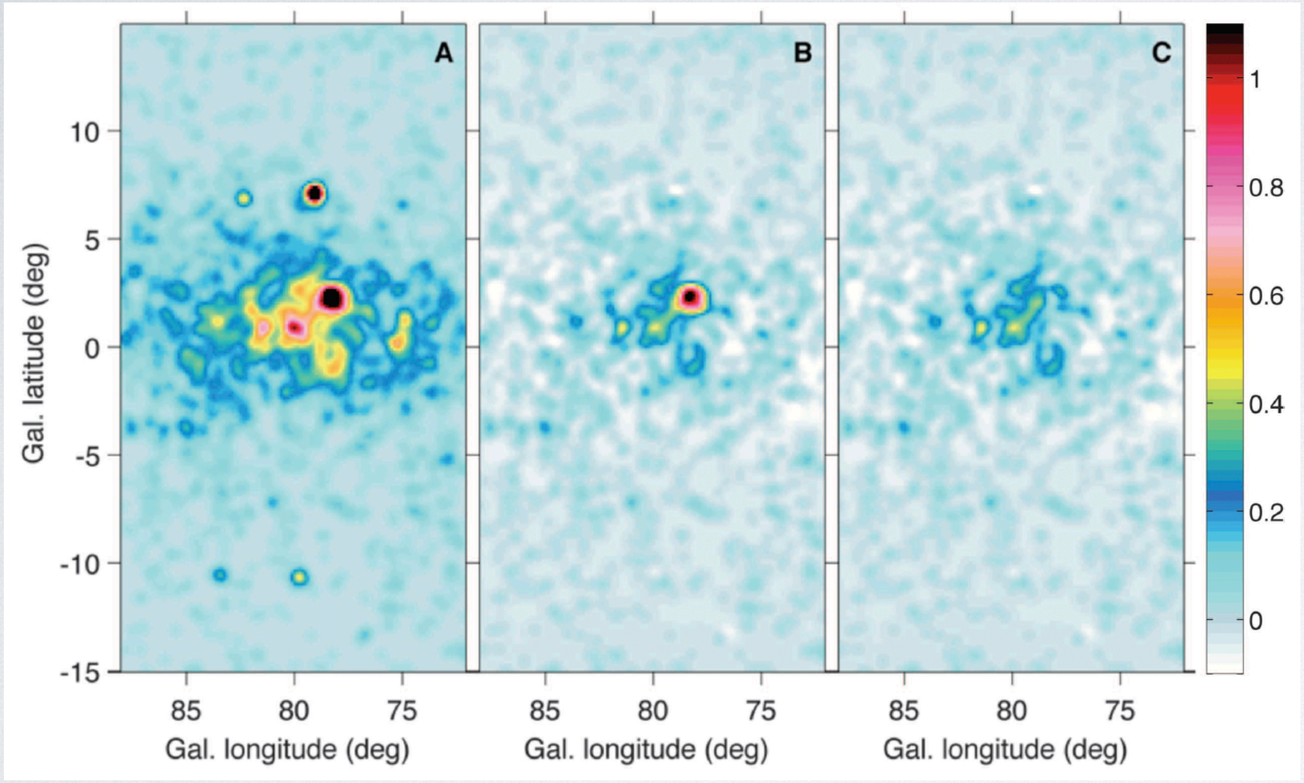

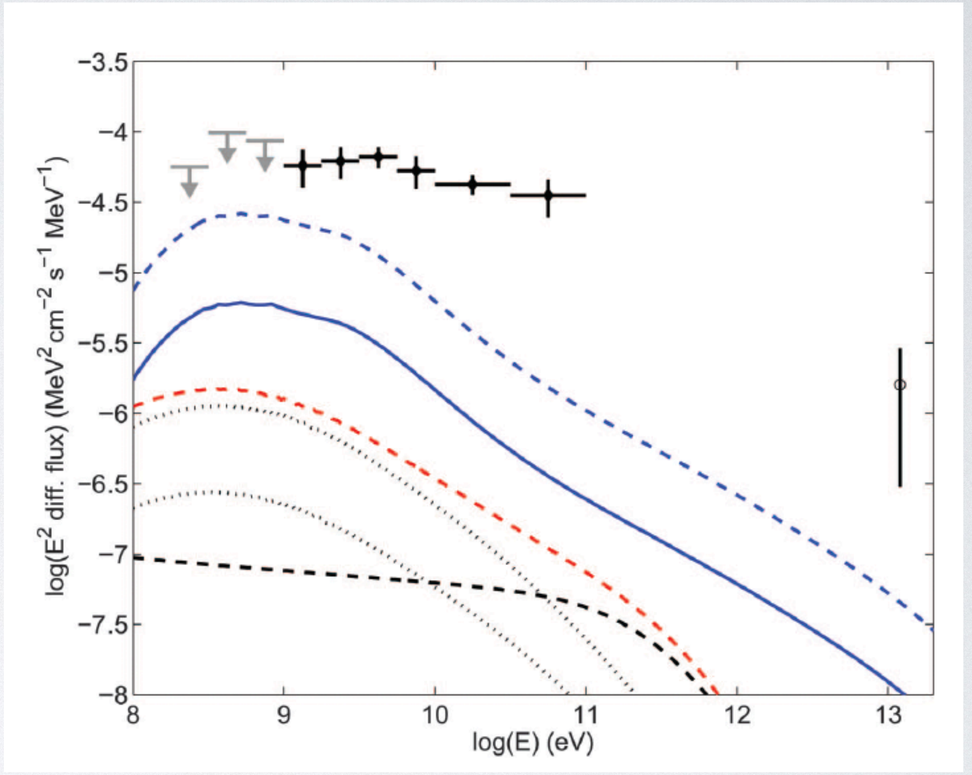

- extended emission up to more than 50 pc (Gaussian sigma/ r39 of 2.0 degrees)
- Hard spectrum in GeV band

ARGO AND HAWC DETECTION

Argo-YBJ Coll. 2014

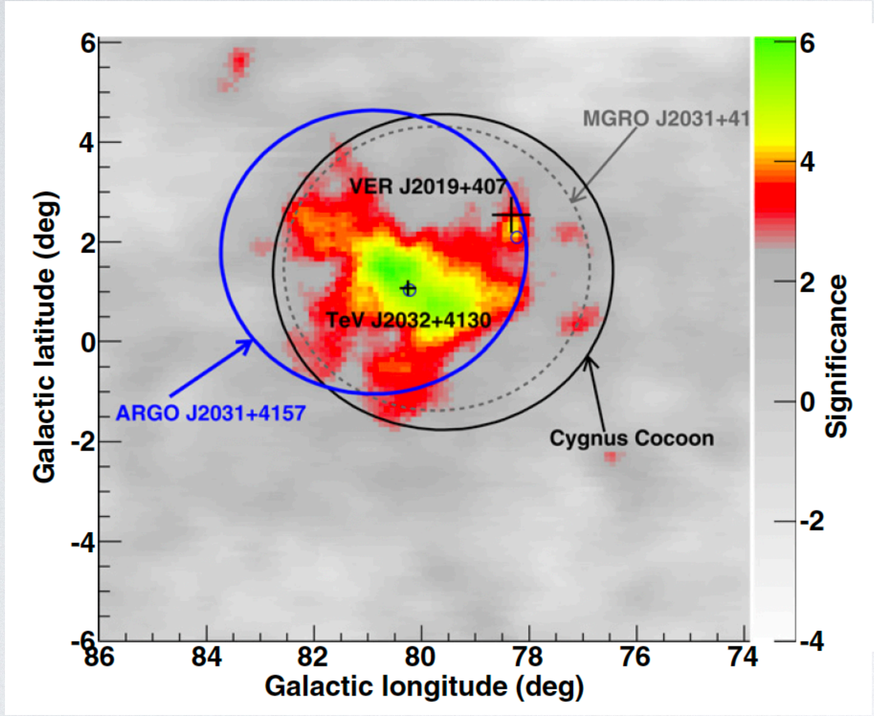

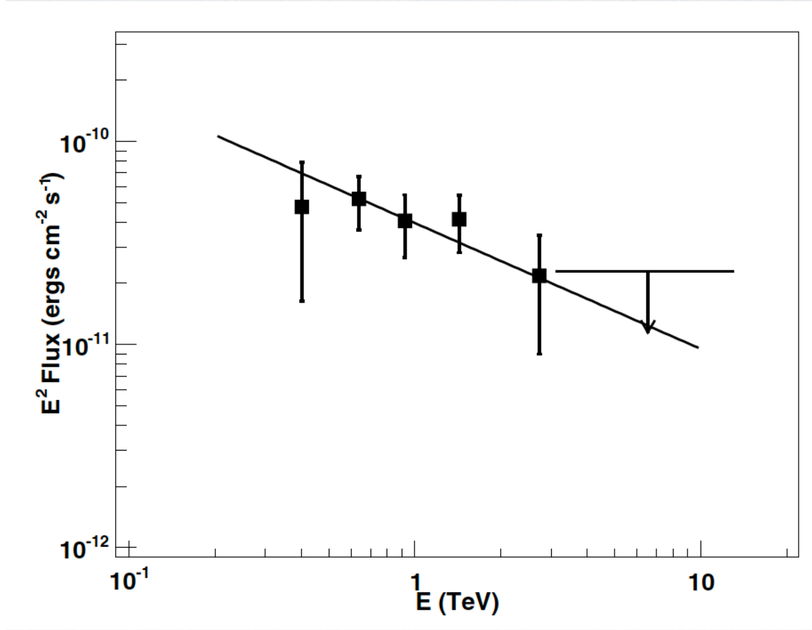

HAWC Coll. 2021

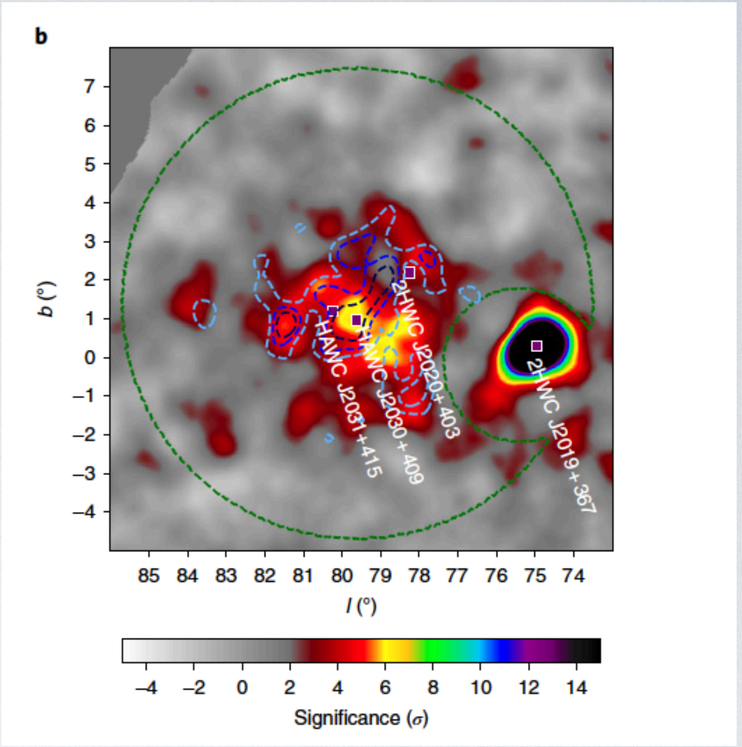

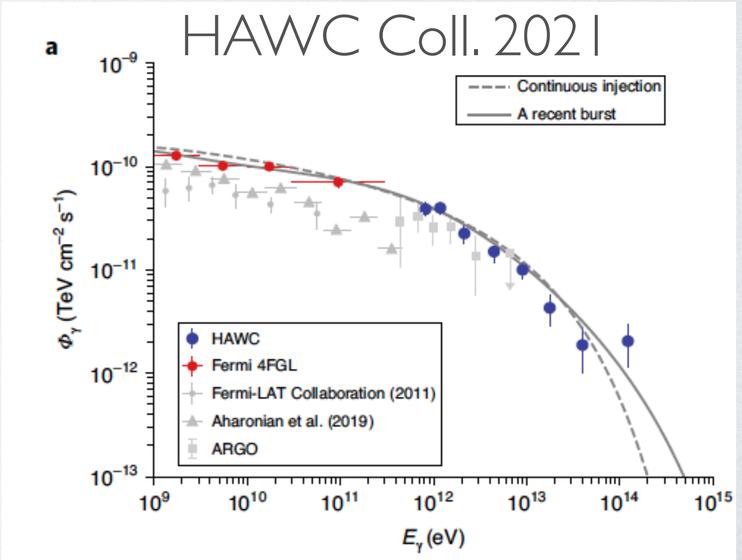

- Similar morphology
- Hard spectrum in GeV band, softening above TeV, up to more than 100 TeV

FERMI LAT 2023 UPDATE

Astiasarain et.al 2023

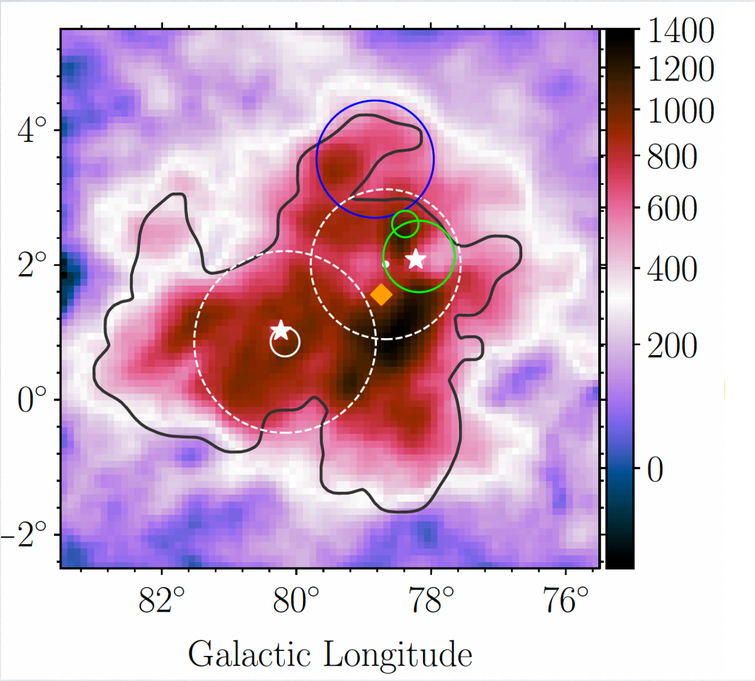

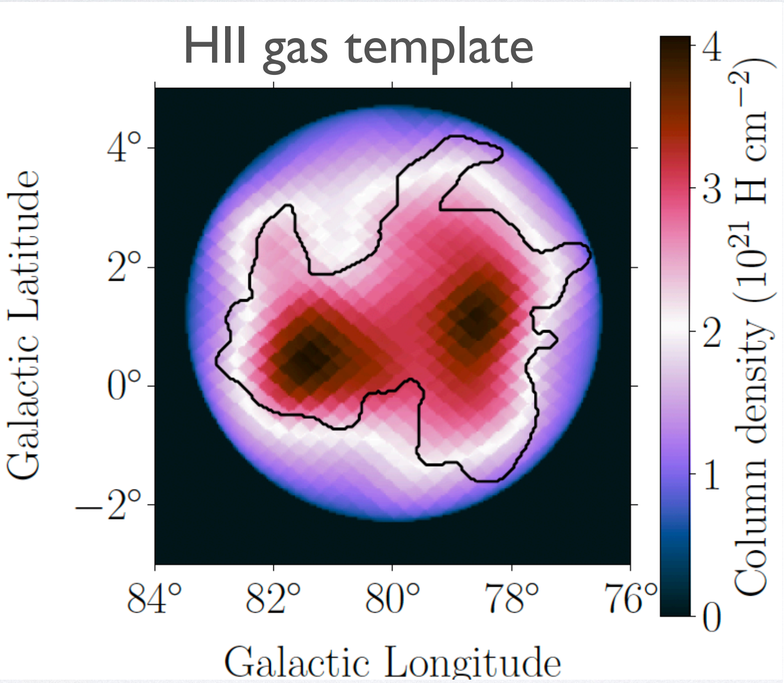

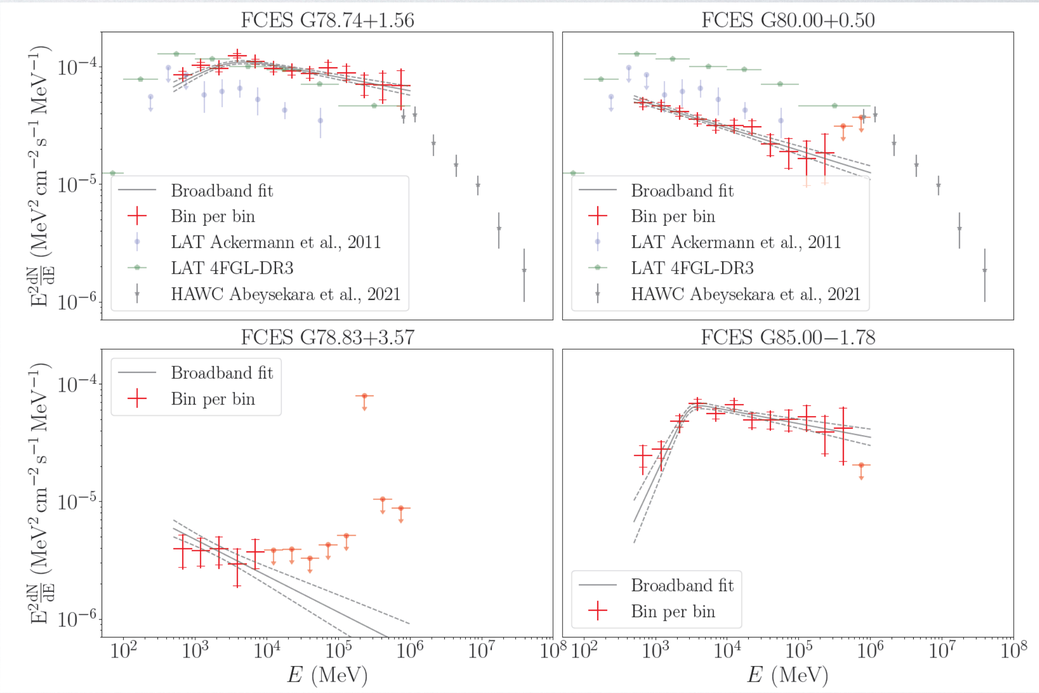

- Slightly more extended (~2.9 degrees)
- multiple component, central extended source with HII gas

LHAASO ADVANTAGES

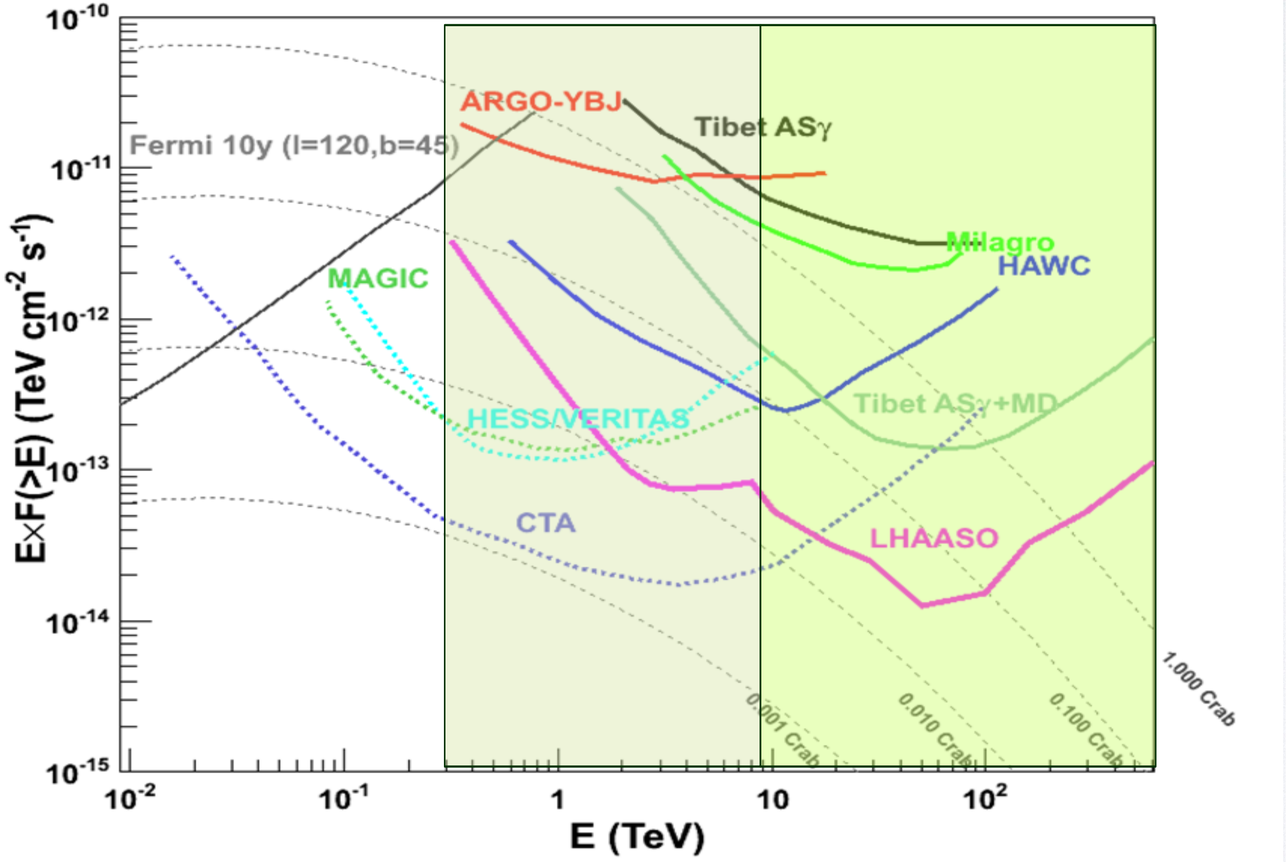

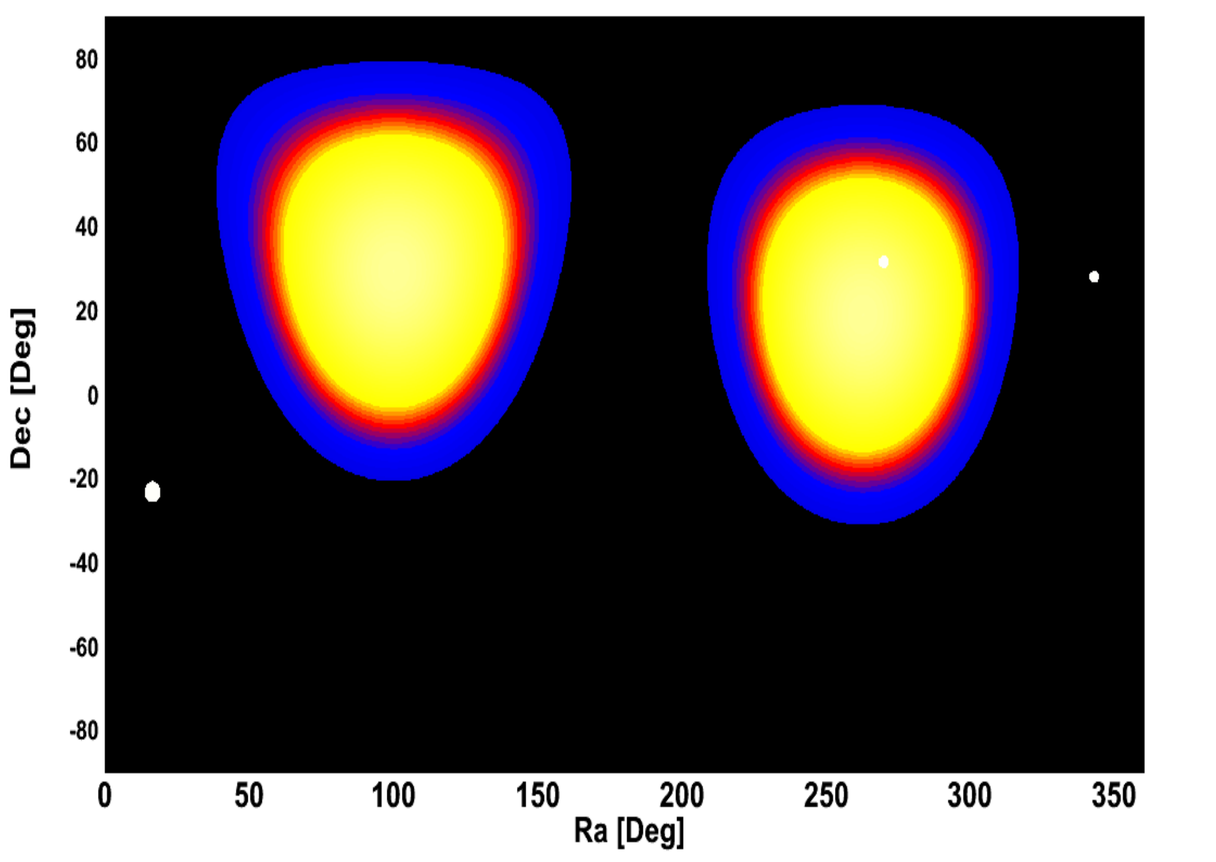

Unprecedented sensitivities above 20 TeV

Large field of view

Hints from first 12 sources

LHAASO Source	Possible Origin	Type	Distance (kpc)	Age (kyr)[a]	L_s (erg/s)[b]	Potential TeV Counterpart[c]
LHAASO J0534+2202	PSR J0534+2200	PSR	2.0	1.26	4.5×10^{38}	Crab, Crab Nebula
LHAASO J1825-1326	PSR J1826-1334	PSR	3.1 ± 0.2[d]	21.4	2.8×10^{36}	HESS J1825-137, HESS J1826-130,
	PSR J1826-1256	PSR	1.6	14.4	3.6×10^{36}	2HWC J1825-134
LHAASO J1839-0545	PSR J1837-0604	PSR	4.8	33.8	2.0×10^{36}	2HWC J1837-065, HESS J1837-069,
	PSR J1838-0537	PSR	1.3[e]	4.9	6.0×10^{36}	HESS J1841-055
LHAASO J1843-0338	SNR G28.6-0.1	SNR	9.6 ± 0.3[f]	$\lesssim 2$[f]	—	HESS J1843-033, HESS J1844-030, 2HWC J1844-032
LHAASO J1849-0003	PSR J1849-0001	PSR	7[g]	43.1	9.8×10^{36}	HESS J1849-000, 2HWC J1849+001
	W43	YMC	5.5[h]	—	—	
LHAASO J1908+0621	SNR G40.5-0.5	SNR	3.4[i]	$\sim 10 - 20$[j]	—	MGRO J1908+06, HESS J1908+063,
	PSR 1907+0602	PSR	2.4	19.5	2.8×10^{36}	ARGO J1907+0627, VER J1907+062,
	PSR 1907+0631	PSR	3.4	11.3	5.3×10^{35}	2HWC 1908+063
LHAASO J1929+1745	PSR J1928+1746	PSR	4.6	82.6	1.6×10^{36}	2HWC J1928+177, 2HWC J1930+188
	PSR J1930+1852	PSR	6.2	2.9	1.2×10^{37}	HESS J1930+188, VER J1930+188
	SNR G54.1+0.3	SNR	$6.3^{+0.8}_{-0.7}$[d]	$1.8 - 3.3$[k]	—	
LHAASO J1956+2845	PSR J1958+2846	PSR	2.0	21.7	3.4×10^{35}	2HWC J1955+285
	SNR G66.0-0.0	SNR	2.3 ± 0.2[d]	—	—	
LHAASO J2018+3651	PSR J2021+3651	PSR	$1.8^{+1.71}_{-1.4}$	17.2	3.4×10^{36}	MGRO J2019+37, VER J2019+368,
	Sh 2-104	H II/YMC	3.3 ± 0.3[m]/4.0 ± 0.5[n]	—	—	VER J2016+371
LHAASO J2032+4102	Cygnus OB2	YMC	1.40 ± 0.08[o]	—	—	TeV J2032+4130, ARGO J2031+4157
	PSR 2032+4127	PSR	1.40 ± 0.08[o]	201	1.5×10^{35}	MGRO J2031+41, 2HWC J2031+415,
	SNR G79.8+1.2	SNR candidate	—	—	—	VER J2032+414
LHAASO J2108+5157	—	—	—	—	—	—
LHAASO J2226+6057	SNR G106.3+2.7	SNR	0.8[p]	~ 10[p]	—	VER J2227+608, Boomerang Nebula
	PSR J2229+6114	PSR	0.8[p]	~ 10[p]	2.2×10^{37}	

LHAASO VIEW ON CYGNUS

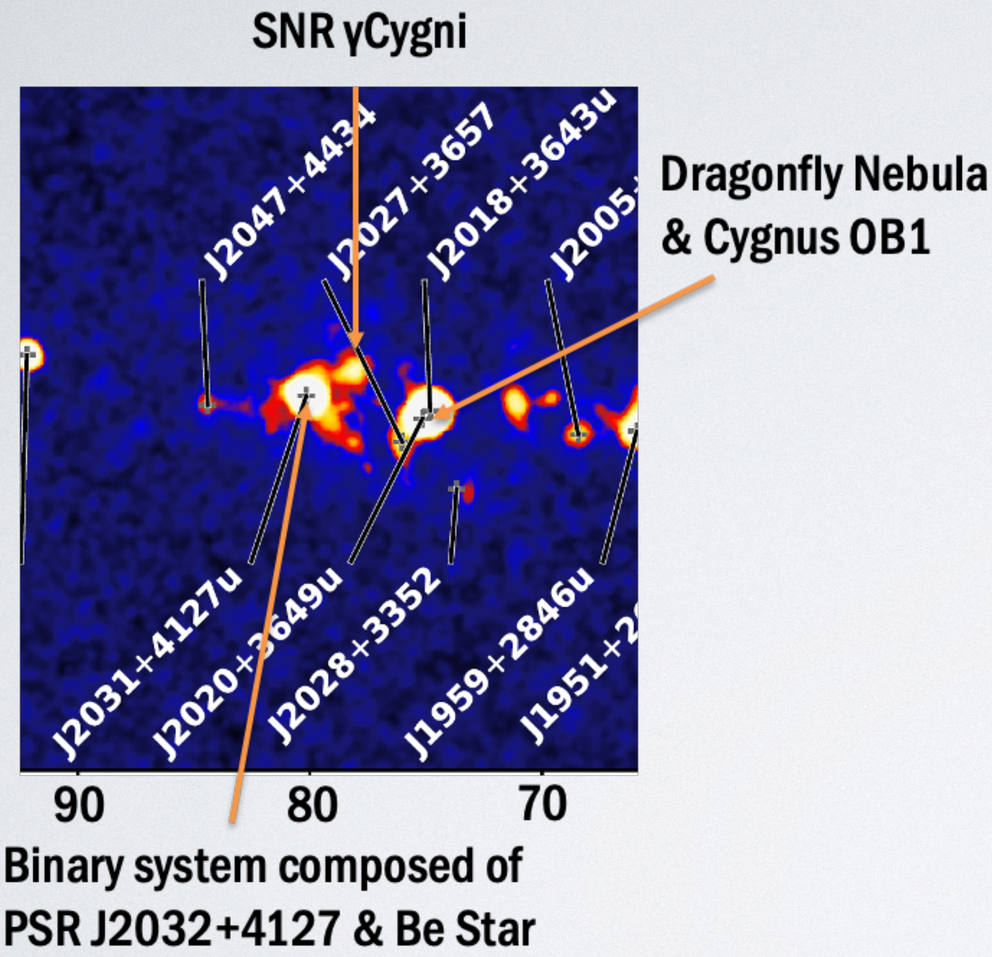

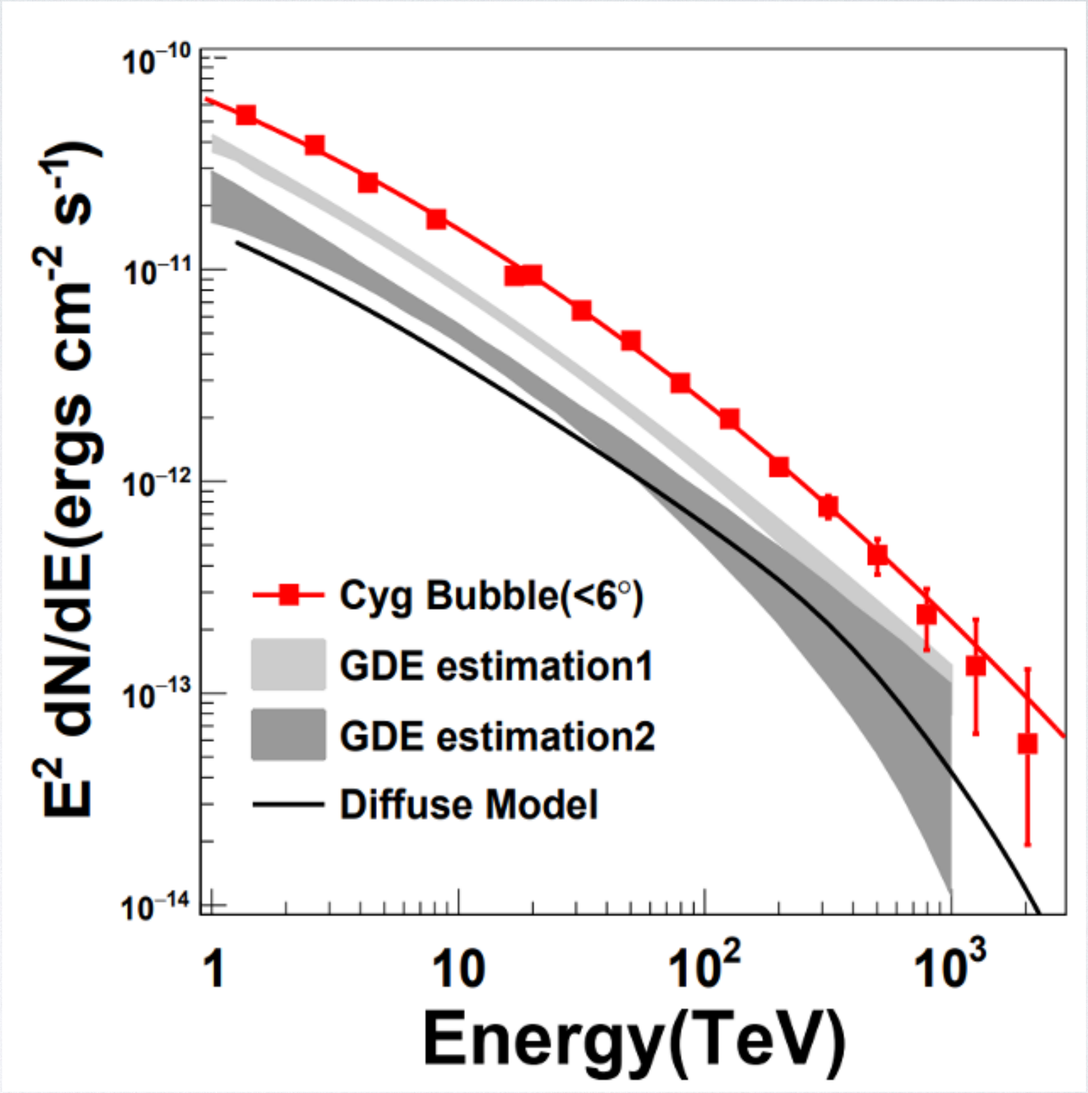

Galactic diffuse gamma-ray background (GDE) must be taken into account

LHAASO VIEW ON CYGNUS

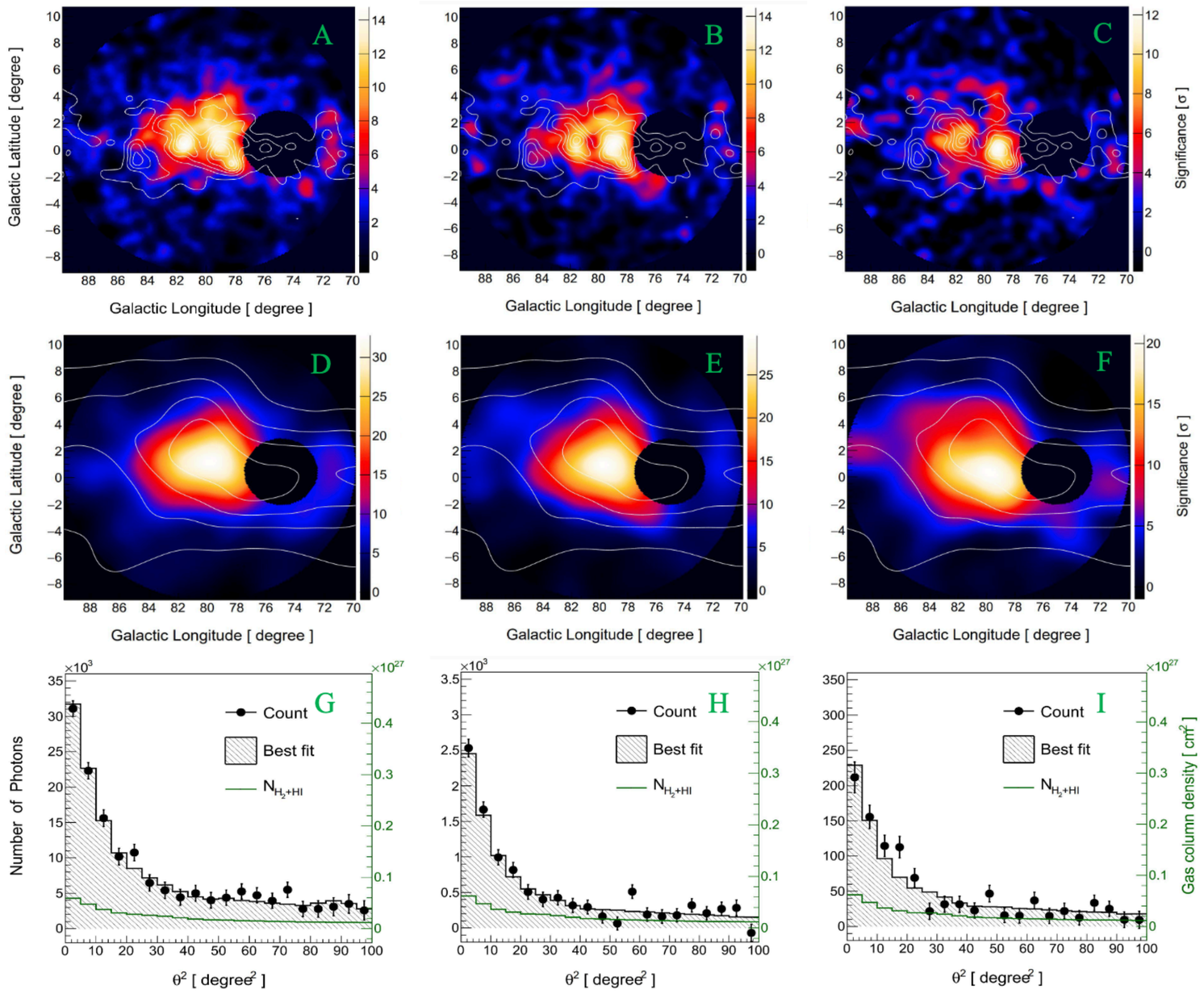

Huge bubble beyond ~10 degrees (200 pc)

LHAASO VIEW ON CYGNUS

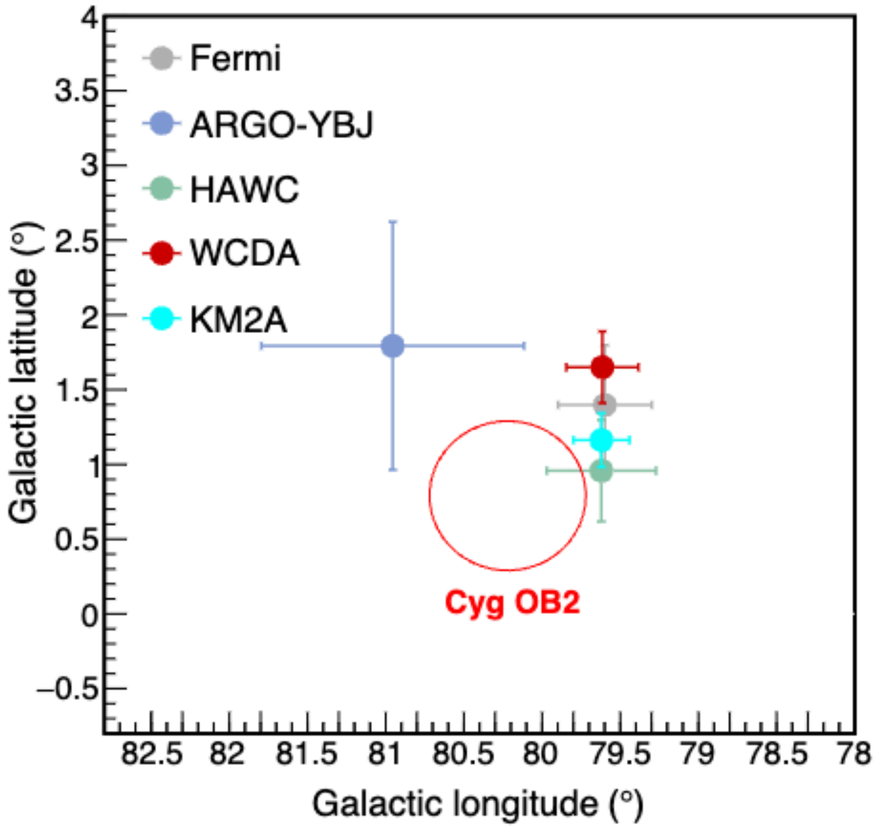

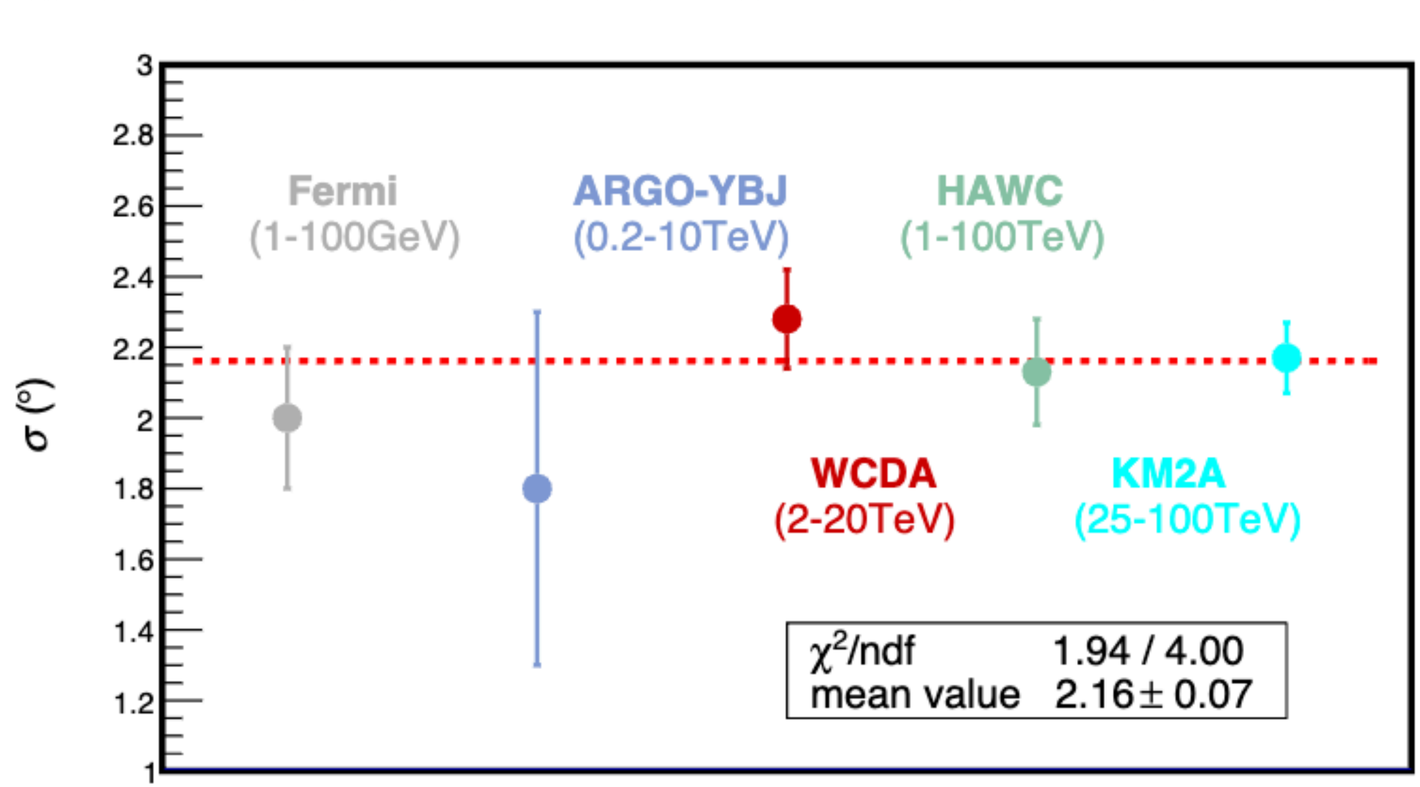

Energy independent morphology
Favor hadronic origin

LHAASO VIEW ON CYGNUS

Source	Components	$\alpha_{2000}(\circ)$	$\delta_{2000}(\circ)$	$r_{39}(\circ)$	TS	$N_0(TeV^{-1}m^{-2}s^{-1})$	Γ
LHAASO J2027+4119	KM2A	307.43 ± 0.16	41.05 ± 0.13	2.17 ± 0.10	145	$(0.62 \pm 0.05) \times 10^{-15}@50TeV$	-2.99 ± 0.07
	WCDA	306.90 ± 0.23	41.33 ± 0.16	2.28 ± 0.14	251.44	$(1.27 \pm 0.14) \times 10^{-9}@7TeV$	-2.63 ± 0.08
HI	KM2A				108	$(0.69 \pm 0.10) \times 10^{-15}@50TeV$	-2.94 ± 0.12
	WCDA				60.77	$(1.43 \pm 0.26) \times 10^{-9}@7TeV$	-2.66 ± 0.12
MC	KM2A				88	$(0.46 \pm 0.06) \times 10^{-15}@50TeV$	-2.87 ± 0.14
	WCDA				67.47	$(1.08 \pm 0.19) \times 10^{-9}@7TeV$	-2.73 ± 0.13
LHAASO J2031+4057	WCDA	307.89 ± 0.09	40.96 ± 0.16	0.33 ± 0.08	115.40	$(0.11 \pm 0.06) \times 10^{-9}@7TeV$	-2.75 ± 0.17

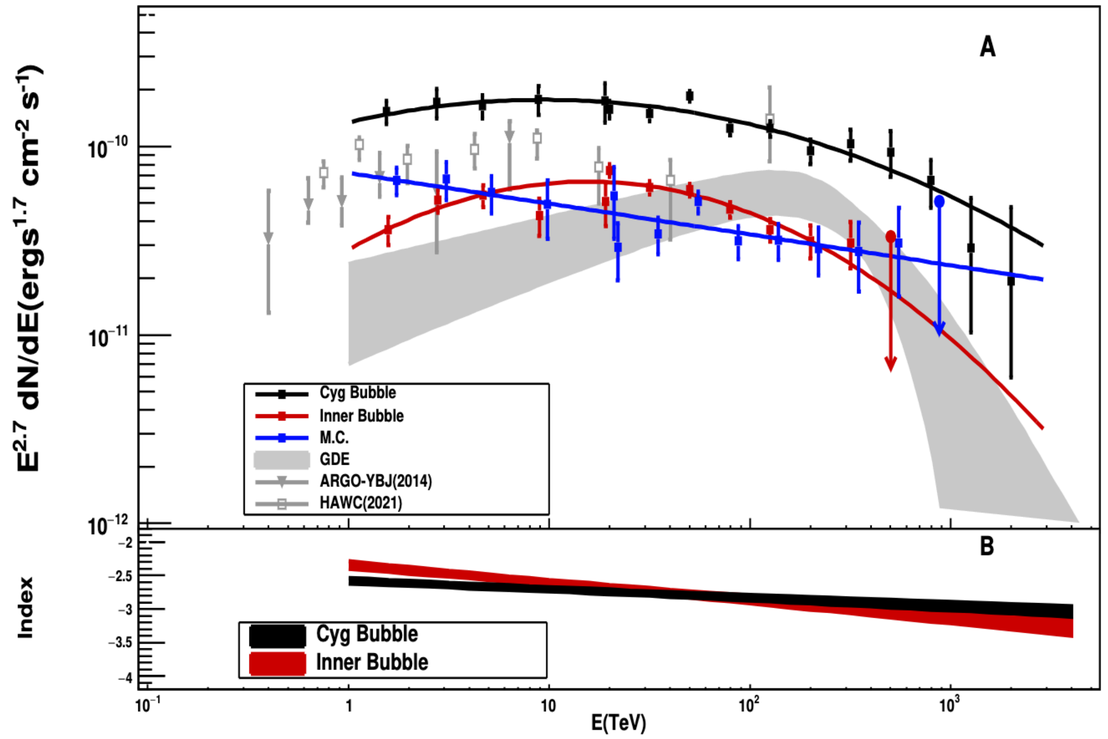

likelihood fitting derived 4 components:

1. inner bubble(Cocoon)
2. Cygnus bubble (~10 degrees, associated with HI gas)
3. Hotspots associated with molecular gas
4. Bright central source

J2032+4127 (PWN/BINARY) are already subtracted from the analysis

Gas distribution and derived CR density

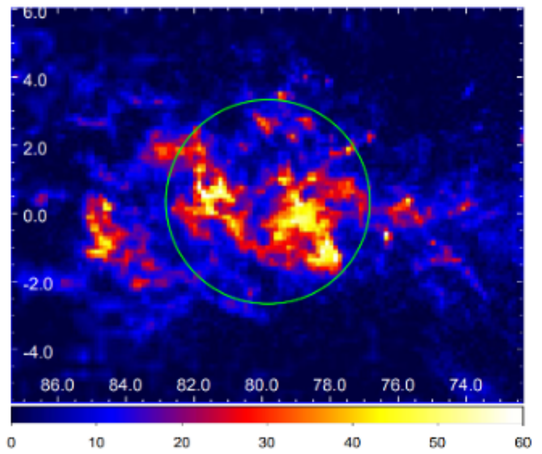

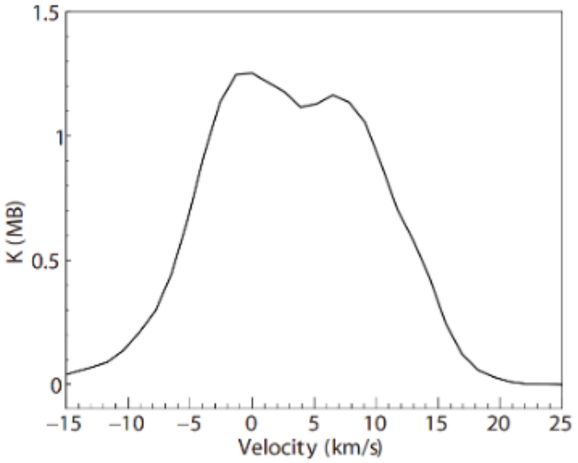

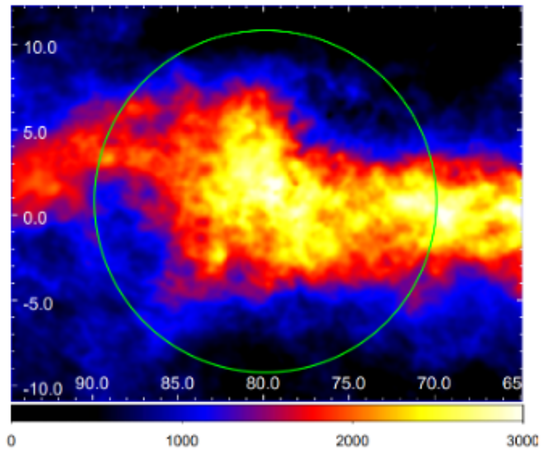

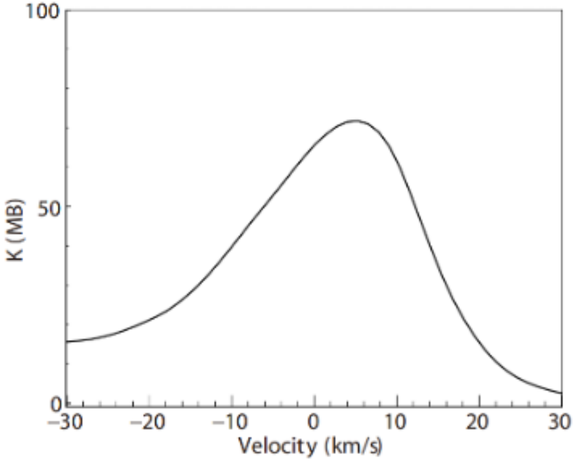

-10 to 20 km/s for CO
-20 to 30 km/s for HI are integrated

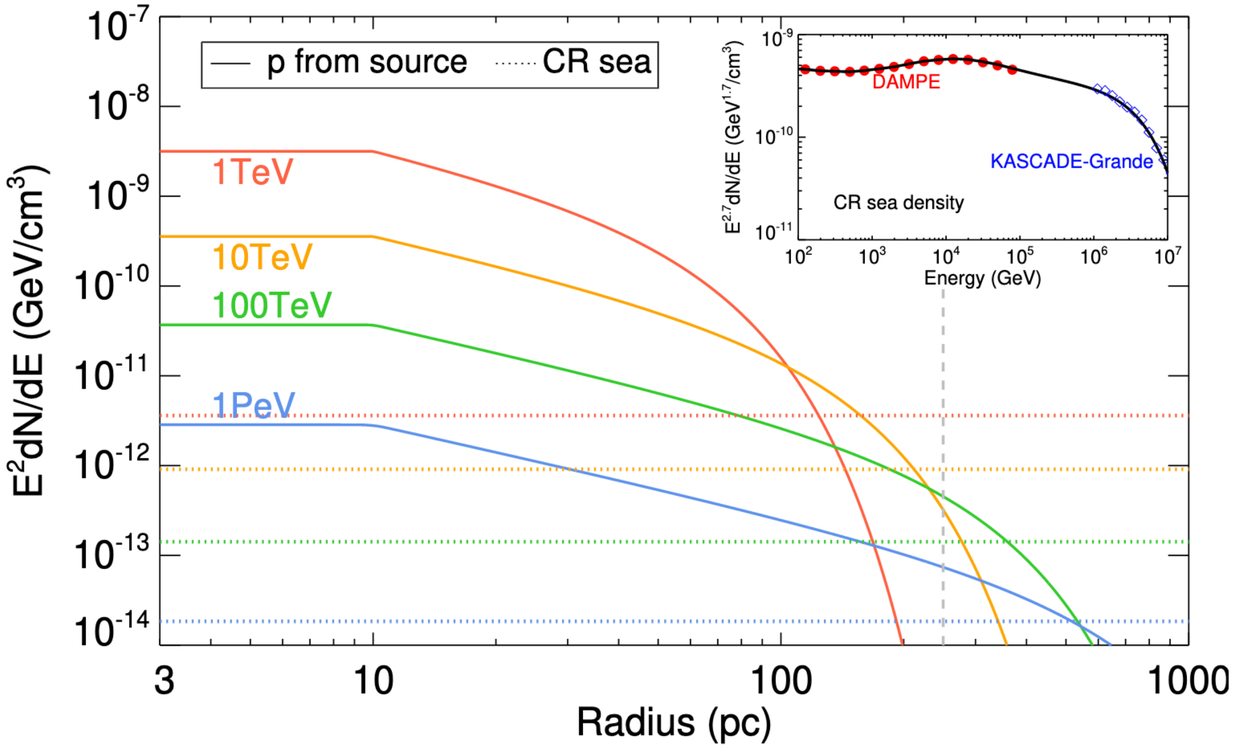

CR injected by the source dominate the CR sea up to several hundred pc

HIGHEST ENETGY PHOTONS

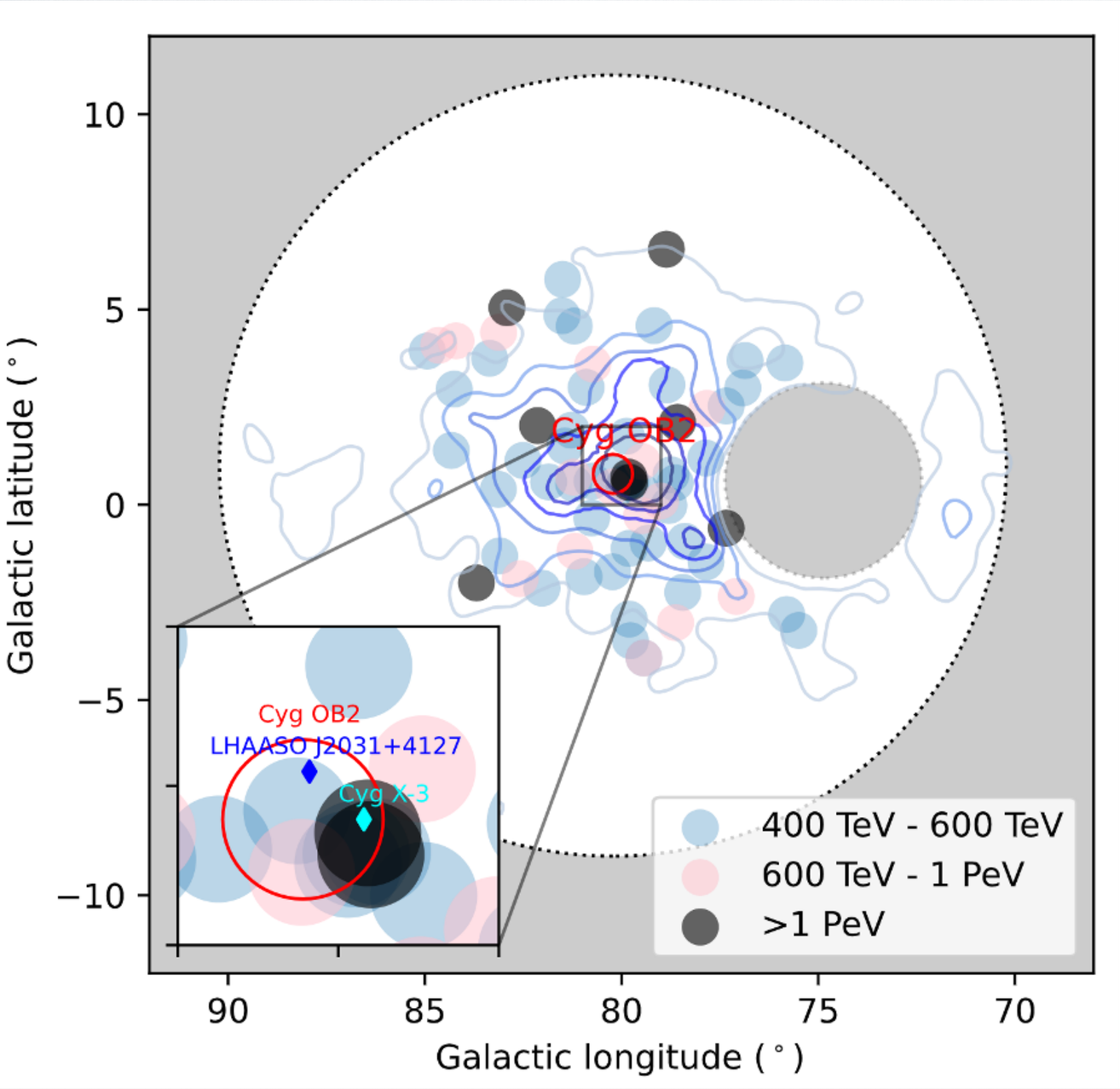

66 photon-like events within a radius of 6 degree with an estimated background of 9.5

7/66 from central 0.5 deg region v.s. 66*(0.5/6)^2≈0.5
2/8 PeV event from central 0.5 deg region

Overdensity at the centre – injection!

E (PeV)	δE (PeV)	N_e	N_μ	$\theta(^\circ)$	$D_{edge}(m)$	$\psi(^\circ)$
1.08	0.16	5904	13.0	19.4	143	4.7
1.19	0.18	5480	14.1	34.4	73	0.2
1.20	0.18	6939	12.6	14.2	132	5.8
1.35	0.20	6938	8.4	27.1	43	2.9
1.38	0.20	6469	8.9	17.4	52	2.6
1.42	0.21	6258	6.6	12.7	57	0.1
1.78	0.27	6665	12.8	18.0	41	1.8
2.48	0.37	13815	29.1	33.0	99	5.2

Schematic fitting of observations

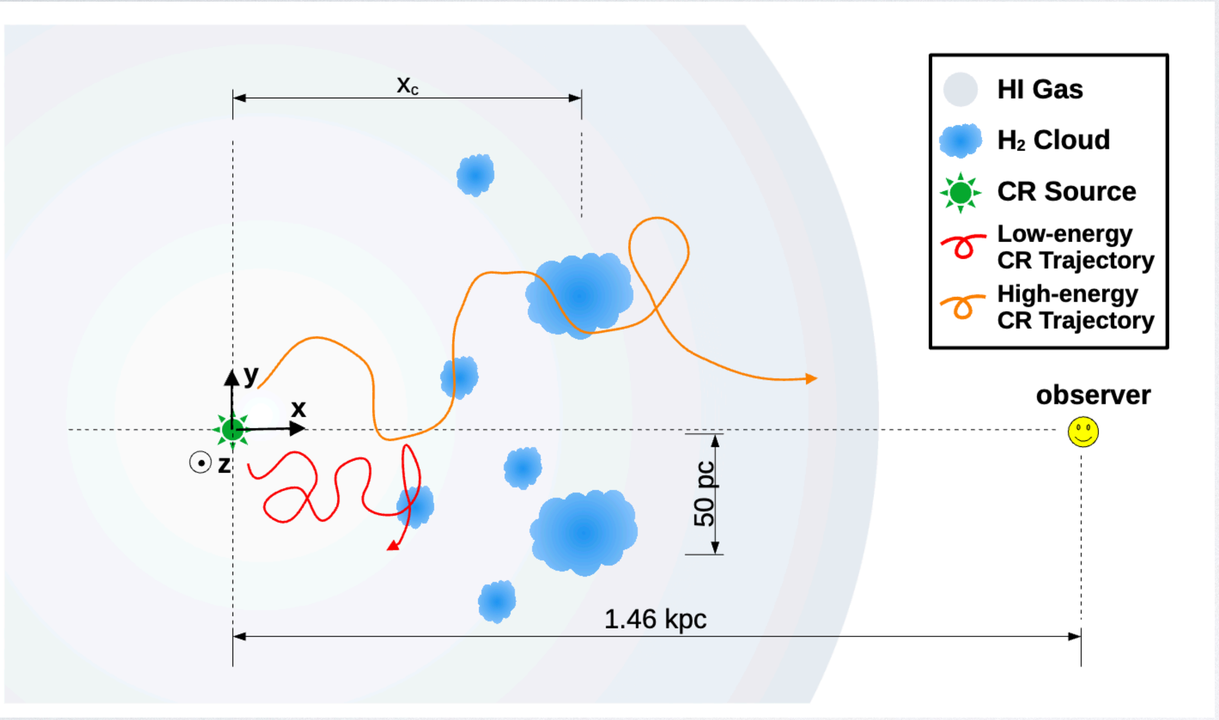

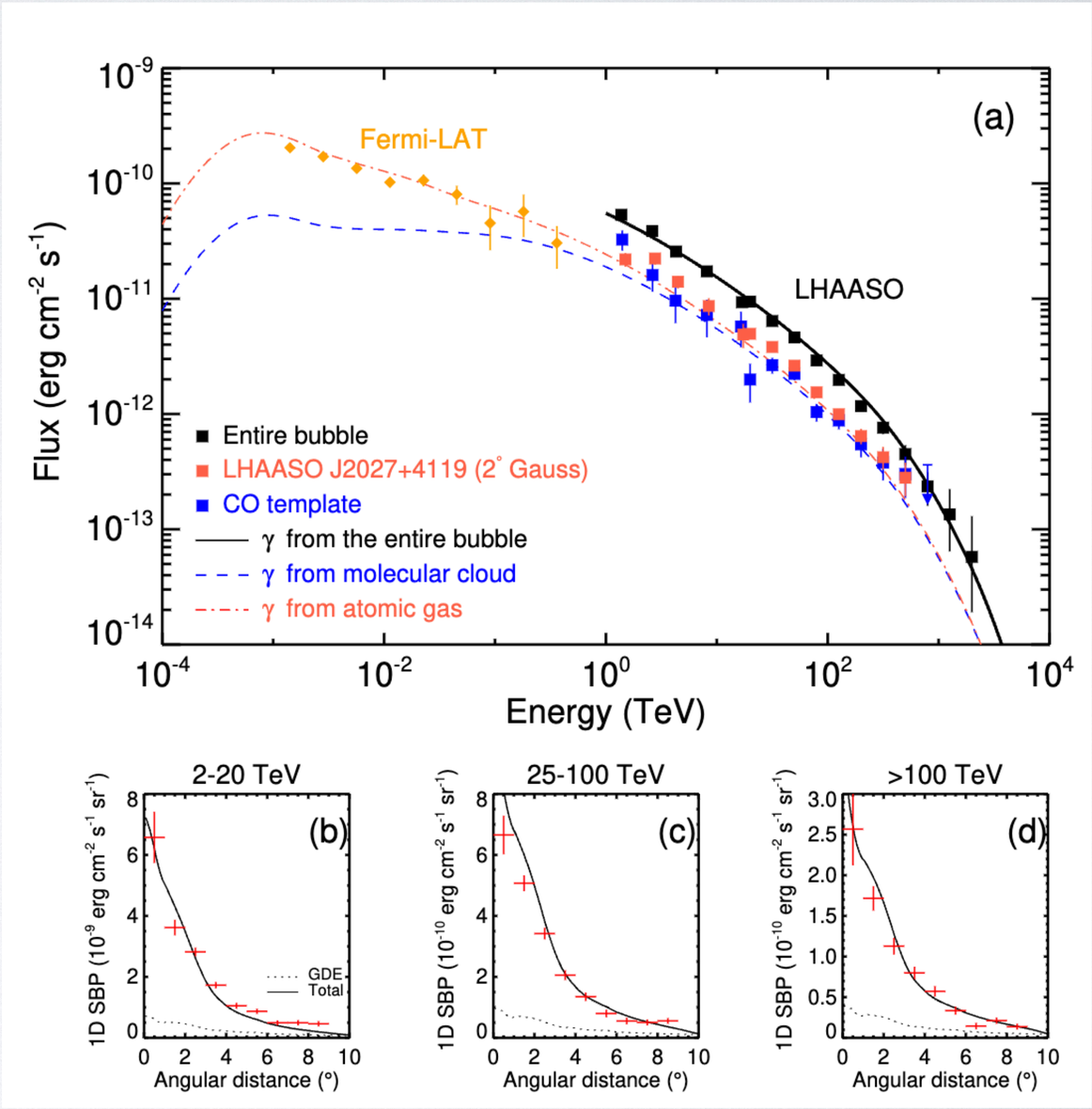

comments:

The inner bubble (cocoon/gaussian) component is **just functional representation** of the data

The similar spectrum reveal same origin of "inner bubble " and Entire bubble

X-ray observations

Guevel et.al 2023

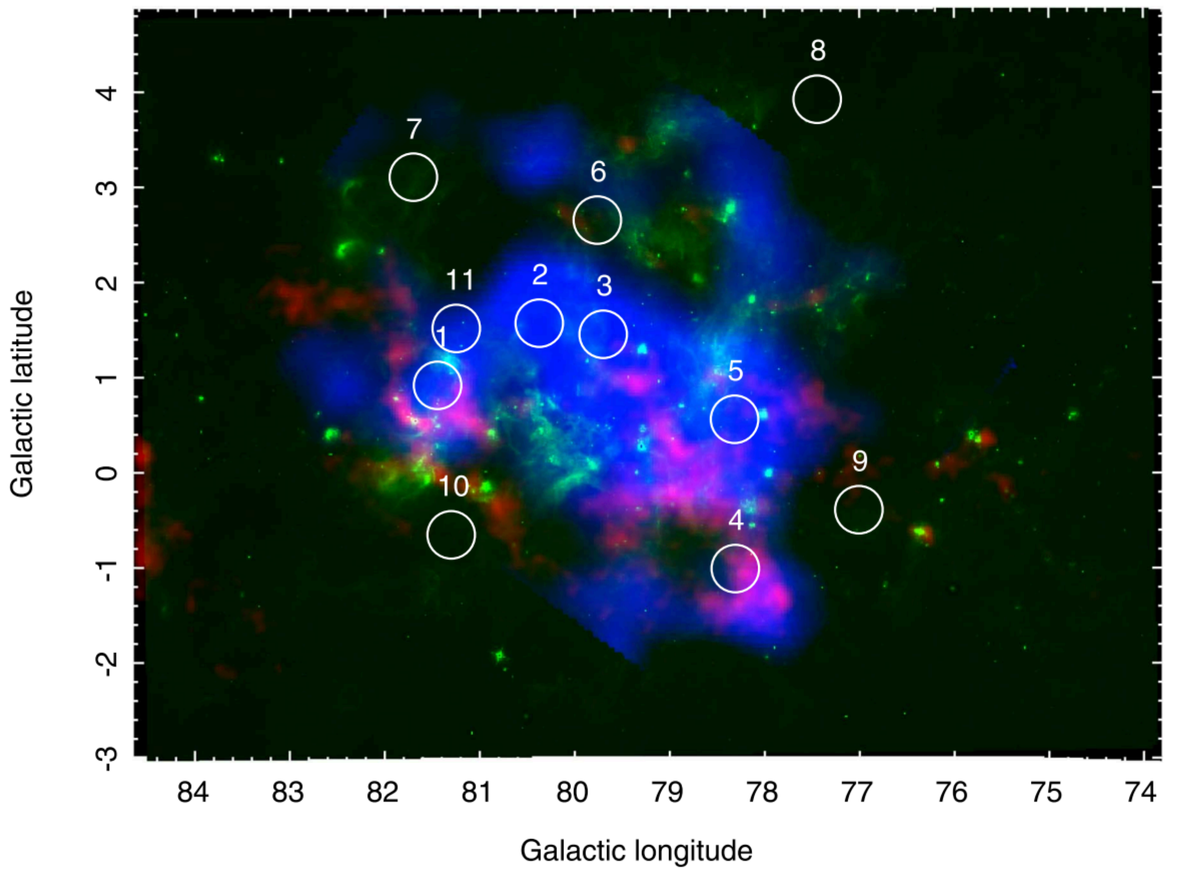

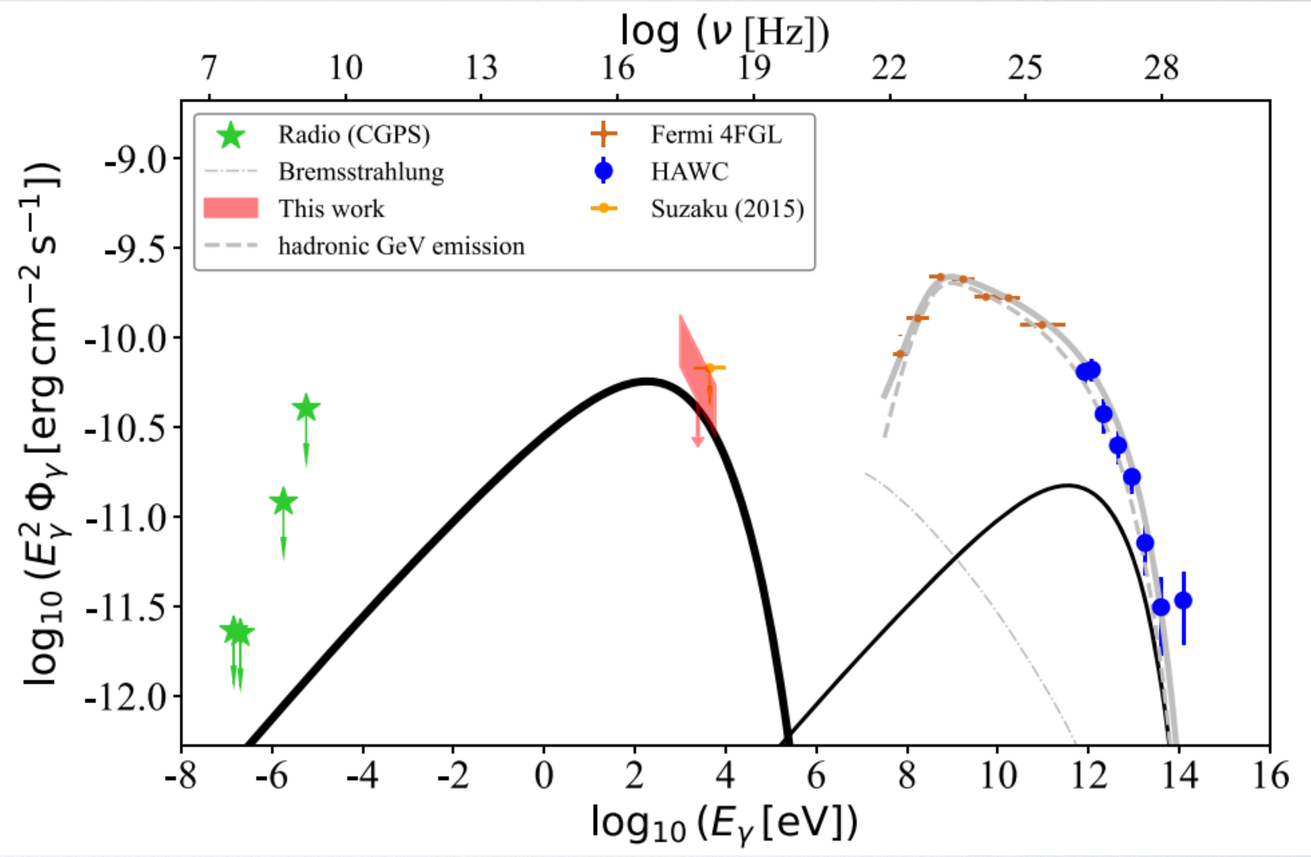

- Swift observations
- at most 1/4 can be of leptonic (B~20muG)

Neutrino searching

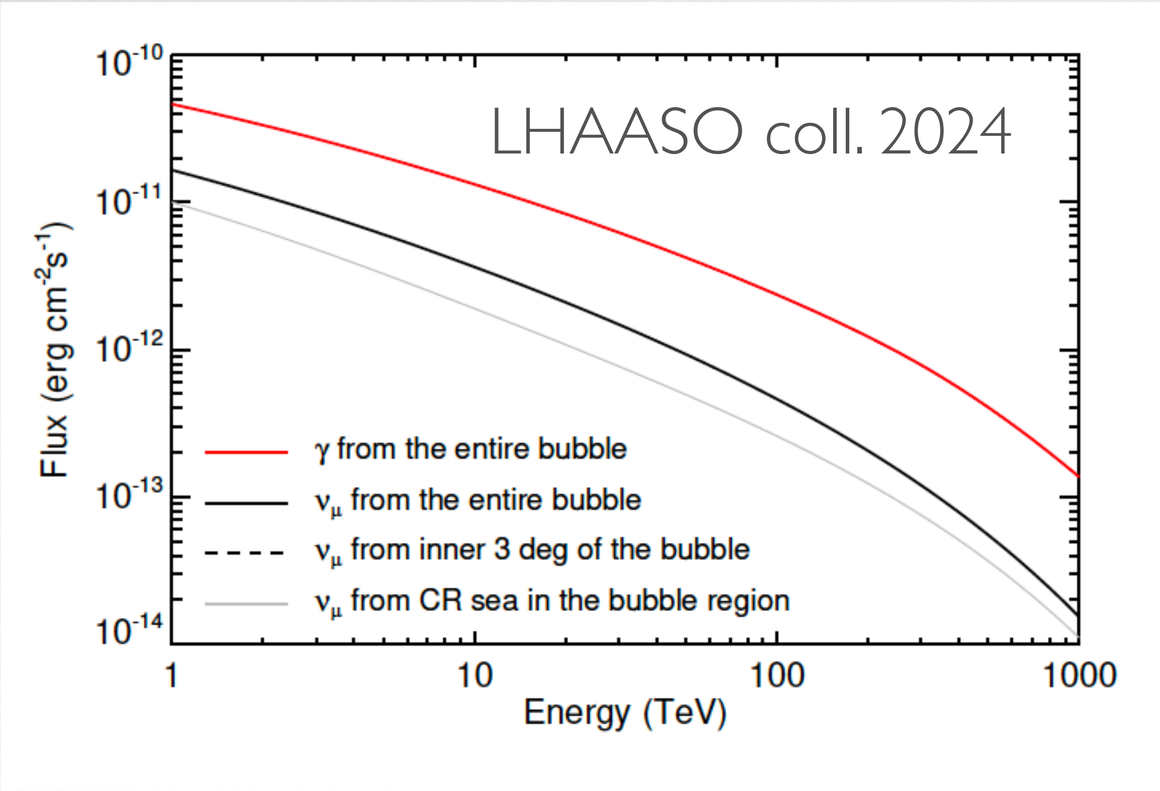

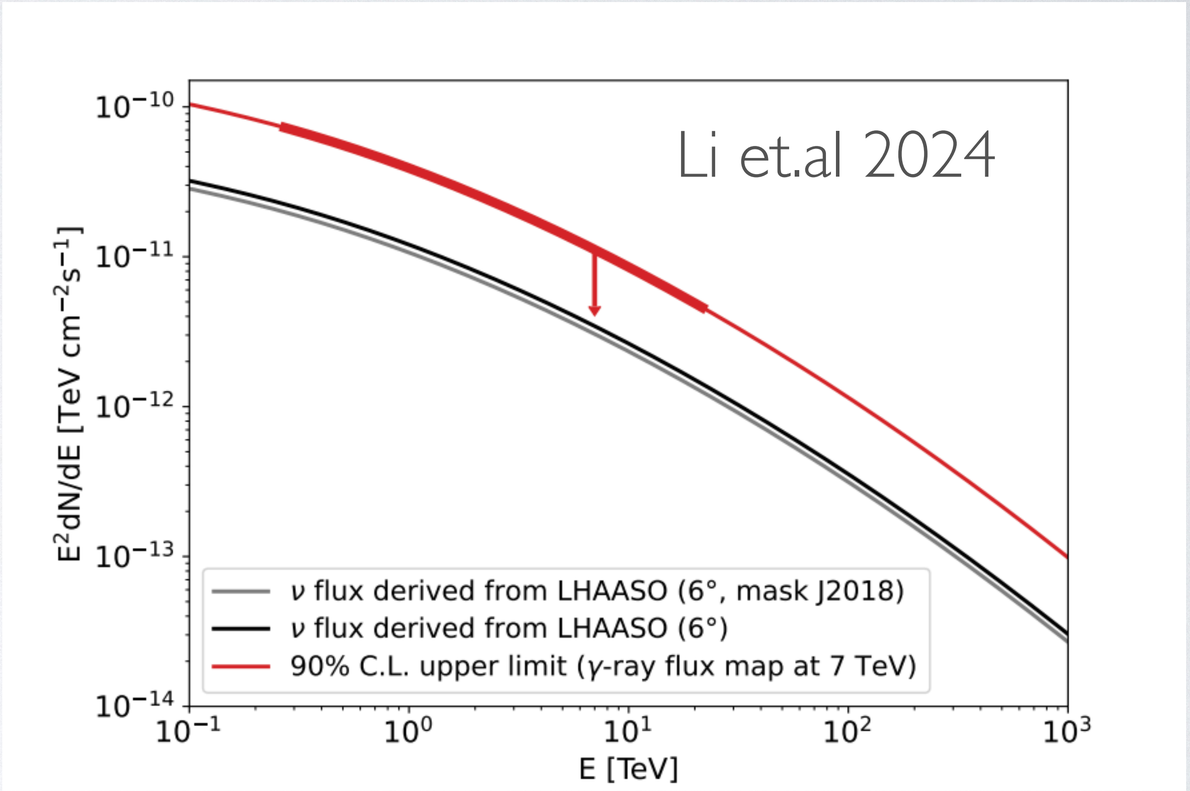

ICECUBE upper limit consistent with prediction

GALACTIC MINI STARBURST W43

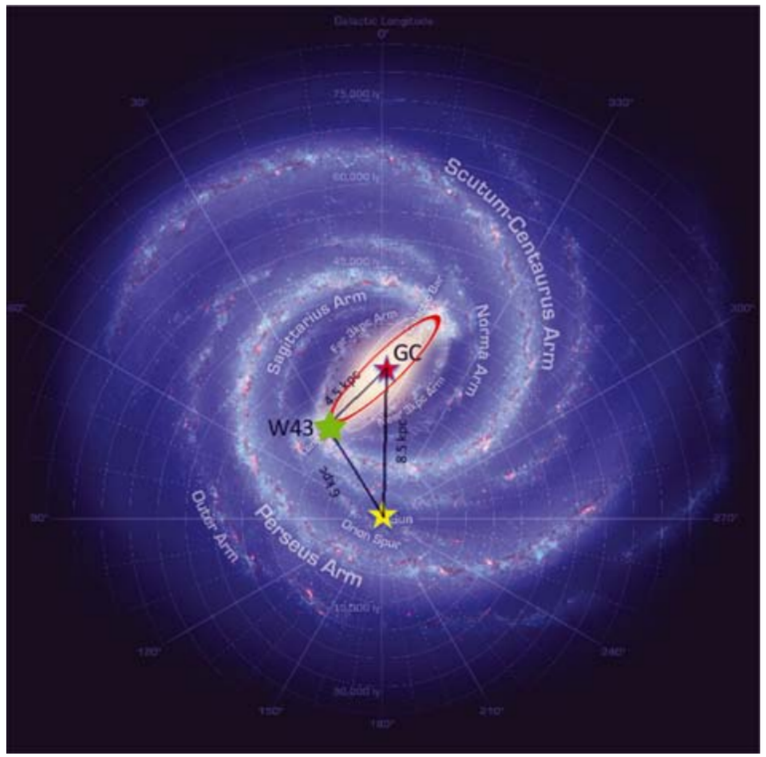

Fig. 9. Artist view of the Galaxy seen face-on with the "long bar" outlined by a red ellipse (Churchwell et al. 2009). W43 is located at the expected transition zone between the bar-dominated region ($R_{GC} < 5$ kpc) and the normal Galactic disk.

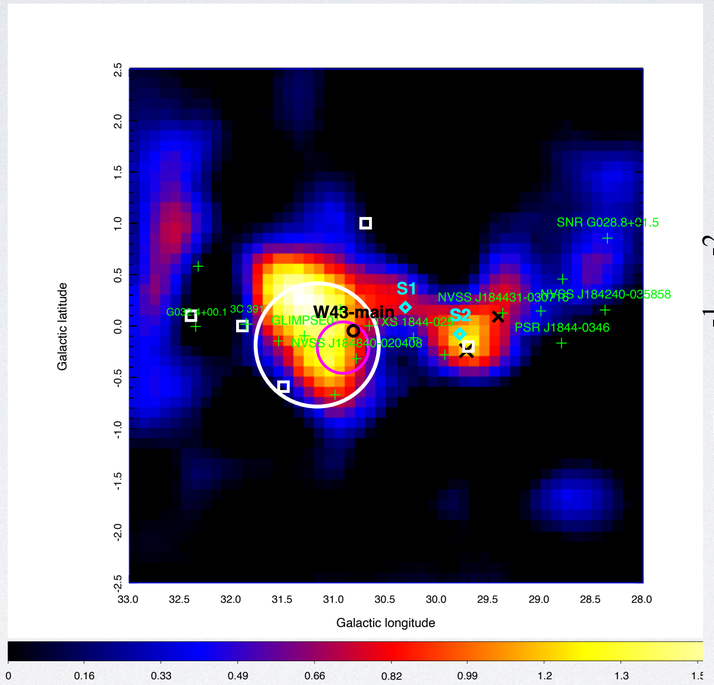

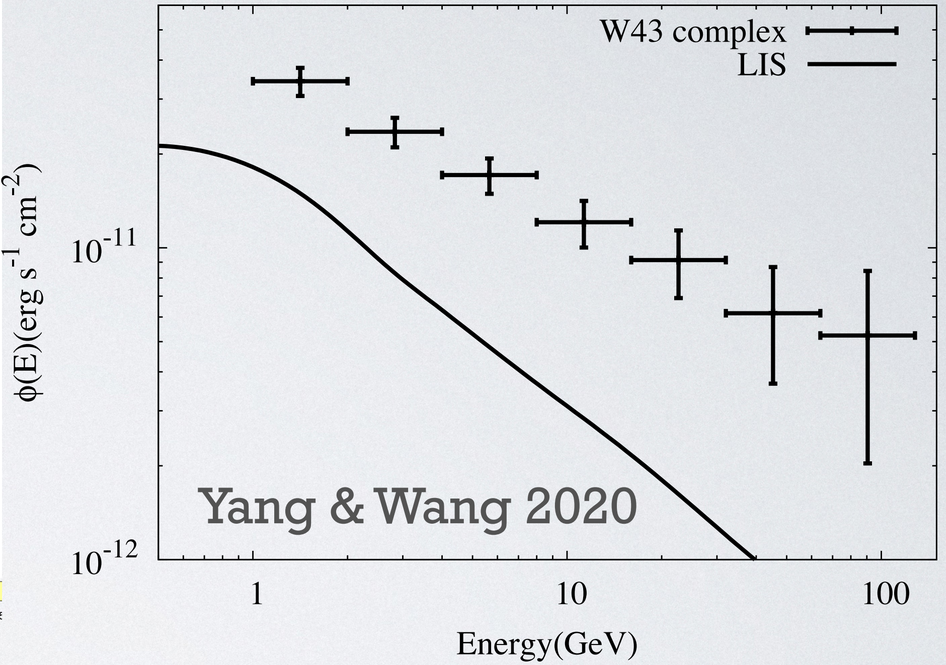

- Galactic mini star burst
- Contribute 10% of the Galactic star formation rate
- Huge HII region excited by central WR/OB cluster
- GeV detection

LHAASO VIEW ON W43

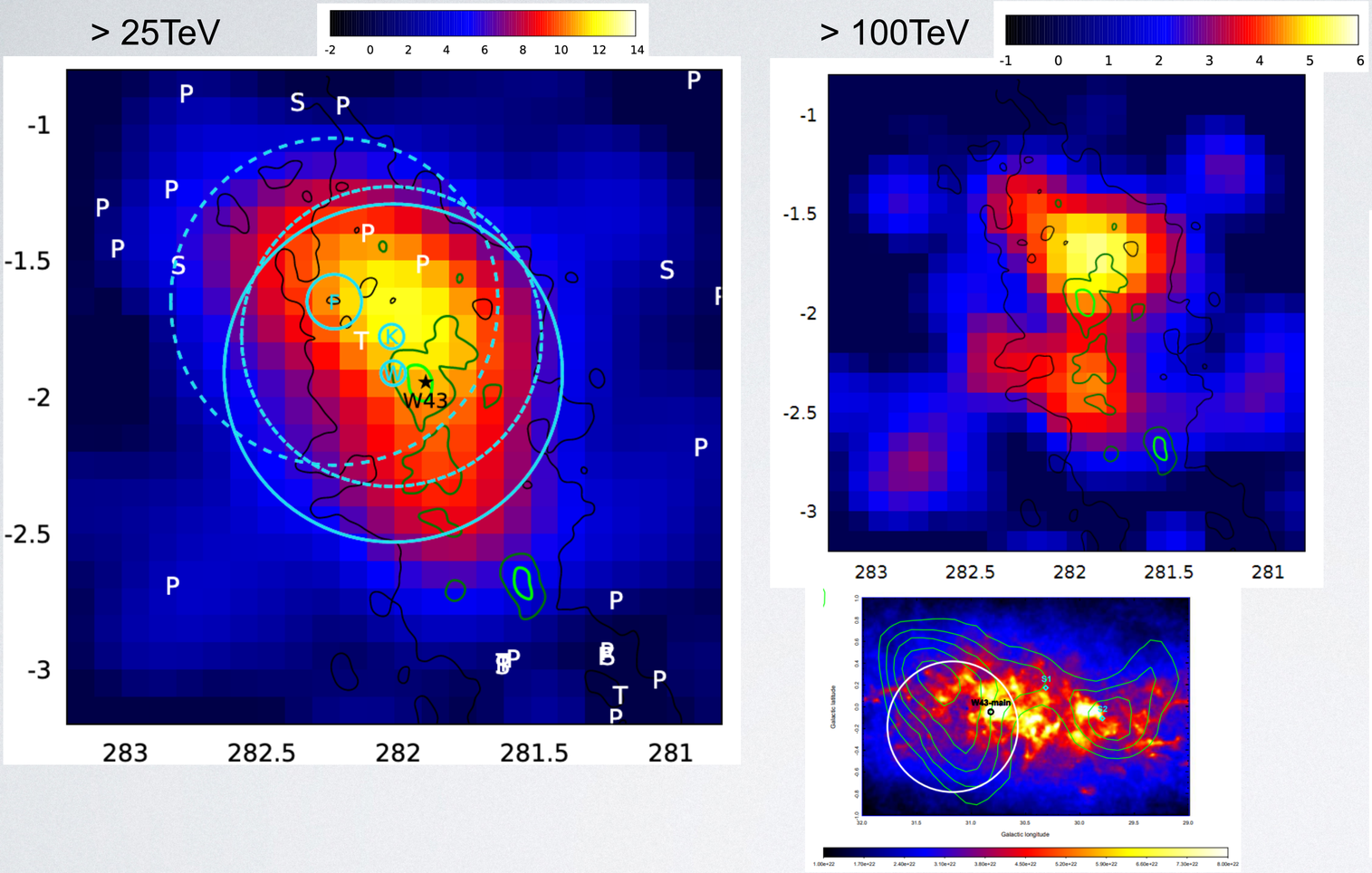

LHAAO Coll.
https://arxiv.org/abs/2408.09905

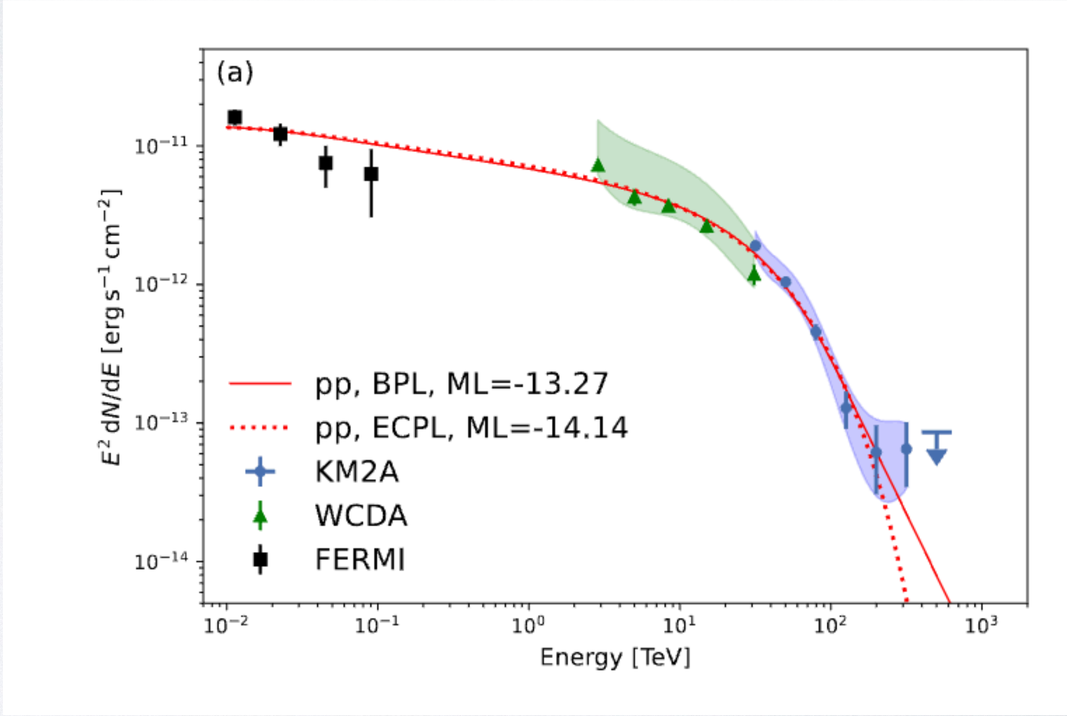

- UHE gamma-ray emission reveal good correlation with dense gas
- Spectrum up to 400 TeV

REMARKS ON LHAASO RESULTS

- Detection of gamma-rays far beyond the "cocoon"
- Central concentration of UHE photons potential injection process
- Curved spectral shape up to PeV (for both 'cocoon' and 'bubble')
- Further analysis with updated 3D gas distribution

LHAASO 高海拔宇宙线观测站 Large High Altitude Air Shower Observatory